Electronic Supplementary Material (ESI) for Inorganic Chemistry Frontiers.

Supporting Information

One-pot Photocatalytic Transformation of Indolines into 3-Thiocyanate Indoles with New Ir(III) Photosensitizers Bearing β-Carbolines

Juan Sanz-Villafruela,[a] Carmen Martínez-Alonso,[a] Igor Echevarría,[a] Mónica Vaquero,[a] Arancha Carbayo,[a] Jairo Fidalgo,[a] Ana M. Rodríguez,[b] José Vicente Cuevas-Vicario,*[a] João C. Lima,[c] Artur J. Moro,[c] Blanca R. Manzano,*[b] Félix A. Jalón,[b] and Gustavo Espino*[a]

Table of Contents

Starting materials and General Methods

Starting materials. $IrCl_3 \times H_2O$ was purchased from Johnson Mattey and used as received. The starting dimer $[Ir(\mu\text{-}Cl)(C\text{^}N)_2]_2$ (C^N = 2-phenylpyridinate, ppy) was prepared according to the reported procedure.[1] The pro-ligand 2-phenylpyridine, triptamine, thiazol-2-carboxaldehyde, 4-methyl-2-thiazolecarboxaldehyde and benzothiazole-2-carboxaldehyde were purchased from Sigma-Aldrich and used without further purification. Deuterated solvents (DMSO-d_6, THF-d_8, CD_3CN, $CDCl_3$) were obtained from Eurisotop. Conventional solvents such as acetonitrile (Fisher Scientific or HPLC, Prolabo), tetrahydrofuran (Acros Organics), anisole (Sigma-Aldrich), dichloromethane (Fisher Scientific), ethanol (Labkem), methyl tert-butyl ether (Scharlau), diethyl ether (Scharlau), acetone (Fisher Scientific) and 2-ethoxyethanol (Acros Organics) were degassed and in some cases distilled prior to be used. Tetrabutylammonium hexafluorophosphate ($[^nBu_4N][PF_6]$) was purchased from Acros Organics.

General Information. All synthetic manipulations were carried out under an atmosphere of dry, oxygen-free nitrogen using standard Schlenk techniques. The solvents were dried and distilled under nitrogen atmosphere before use. Elemental analyses were performed with a Thermo Scientific Flash 2000 Elemental Microanalyzer. In some cases, the data were reasonably accurate, but in others, the agreement of calculated and found values for carbon was > 0.4%, so that solvent molecules were introduced in the molecular formulae to improve agreement. IR spectra were recorded on a Jasco FT/IR-4200 spectrophotometer (4000–400 cm^{-1} range) with Single Reflection ATR Measuring Attachment. UV-Vis absorption spectra were measured in a Shimadzu UV-2450 spectrophotometer. Fluorescence steady-state and lifetime measurements were performed in a FLS980 (Edinburg Instruments) Fluorimeter with Xenon Arc Lamp 450W and TCSPC laser, respectively. Quantum Yield was determined by using in a FLS980 (Edinburg Instruments) with Xenon Arc Lamp 450W and Red PMT Sphere as detector. HR-ESI(+) Mass spectra (position of the peaks in Da) of ligands and Ir(III)-complexes were recorded with an Agilent LC-MS system (1260 Infinity LC / 6545 Q-TOF MS spectrometer) using DCM/DMSO (4:1) as the sample solvent and (0.1%) aqueous HCOOH/MeOH as the mobile phase. The experimentally obtained *m/z* values are expressed in Da and the isotopic distribution matches that of calculated fragments LCI-MS of the isolated organic thyocianates were recorded with an Agilent 6890N system (Micromass AutoSpec (Waters)/LSIMS/ Triple sector (EBE)). NMR samples were prepared by dissolving the suitable amount of compound in 0.5 mL of the respective deuterated solvent and the spectra were recorded at 298 K on a Varian Unity Inova-400 (399.94 MHz for ^1H; 376.29 MHz for ^{19}F; 100.6 MHz for ^{13}C) and BRUKER AVANCE III HD 300 MHz. Typically, ^1H NMR spectra were acquired with 32 scans into 32 k data points over a spectral width of 16 ppm. ^1H and $^{13}C\{^1H\}$ chemical shifts were internally referenced to TMS via the residual ^1H and ^{13}C signals of CHD_2SOCD_3 (δ = 2.50 ppm and δ = 39.52 ppm), $CHCl_3$ (δ = 7.26 ppm), CHD_2CN (δ = 1.94 ppm) for CD_3SOCD_3, $CDCl_3$ and CD_3CN respectively, according to the values reported by Fulmer et al.[2] Chemical shift values (δ) are reported in ppm and coupling constants (J) in Hertz. The splitting of proton resonances in the reported ^1H NMR data is defined as s = singlet, d = doublet, t = triplet, m = multiplet, bs = broad singlet. 2D NMR spectra such as ^1H-^1H gCOSY, ^1H-^1H NOESY, ^1H-^{13}C gHSQC and ^1H-^{13}C gHMBC were recorded using standard pulse sequences. The probe temperature (±1 K) was controlled by a standard unit calibrated with methanol as a reference. All NMR data processing was carried out using MestReNova version 10.0.2.

X-ray Crystallography. A summary of crystal data collection and refinement parameters for **[IrL2]Cl·0.5CH_2Cl_2** and **[IrL3]Cl·0.5CH_3OH·0.75H_2O** are given in Table S1. Single crystals of compounds were coated in high-vacuum grease, mounted on a glass fiber, and transferred to a Bruker SMART APEX CCD-based diffractometer equipped with a graphite monochromated Mo-Kα radiation source (λ = 0.71073 Å) for **[IrL2]Cl·0.5CH_2Cl_2** and Cu-Kα (λ = 1.5417 Å) for **[IrL3]Cl·0.5CH_3OH·0.75H_2O**. The highly redundant datasets were integrated using SAINT[3] and corrected for Lorentz and polarization effects. The absorption correction was based on the function fitting to the empirical transmission surface as sampled by multiple equivalent measurements with the program SADABS.[4]

The software package WINGX[5,6] was used for space group determination, structure solution, and refinement by full-matrix least-squares methods based on F^2. A successful solution by direct methods provided most non-hydrogen atoms from the E-map. The remaining non-hydrogen atoms were located in an alternating series of least-squares cycles and difference Fourier maps. All non-hydrogen atoms were refined with anisotropic displacement coefficients. Hydrogen atoms were placed using a "riding model" and included in the refinement at calculated positions. CCDC reference numbers for **[IrL2]Cl·0.5CH_2Cl_2** and **[IrL3]Cl·0.5CH_3OH·0.75H_2O** are 2038307 and 2038308.

Measurements of UV-Vis Absorption and photoluminescence Spectra

UV-Vis absorption spectra were recorded in the 200-1100 nm spectral range by a Shimadzu UV-2450 spectrophotometer, using 10 mm quartz cells, while excitation and emission spectra were recorded on a FLS980 spectrofluorometer (from Edinburgh Instruments) equipped with triple grating turret monochromators and a Red PMT Sphere detector. The F980 spectrometer operating software was used to collect and process fluorescence data. Samples of $1 \cdot 10^{-5}$ M solutions in CH_3CN were prepared and deoxygenated in a Schlenk using Freeze-Pump-Thaw technique. Then, the solutions were kept under inert atmosphere in quartz cuvettes equipped with Teflon septum screw caps for all the luminescence measurements. All optical measurements were made at room temperature.

The luminescence emission spectra were recorded by exciting at 405 nm with a Xenon Arc lamp and the maximum emission wavelength was measured from 420 to 800 nm. The photoluminescence quantum yields (PLQY or Φ) were calculated by detecting all sample emission through the use of an integrating sphere. For the determination of the luminescence lifetime of compounds **[IrL1]Cl-[IrL3]Cl**, the fluorescence decay was measured on a FLS980 spectrofluorometer equipped with a TSCPC laser and a REDPMT detector. The F980 spectrometer operating software was used to collect and process luminescence lifetime data. The instrumental parameters used were as follows: λ_{ex} = 405 nm, $\Delta\lambda_{ex}$ = 0.2 nm, λ_{em} = 648 nm, $\Delta\lambda_{em}$ = 4 nm, 2000 channels, integration time = 1 μs, iris setting = 100.

Electrochemical measurements: Electrochemical measurements were performed using a portable potentiostat/galvanostat PalmSens3 (PalmSens) equipment controlled by the software PSTrace4 Version 4.4.2. All experiments were carried out using a three-electrode cell with a glassy carbon-disc (diameter = 3 mm) as the working electrode, a platinum-wire as the auxiliary electrode, and a Ag/AgCl (MF-2052 BASi) reference electrode separated from the bulk solution by a Vycor™ frit. Oxygen was removed from the solution by bubbling argon for 10 minutes and keeping the current of argon along the whole experiment. The measurements were recorded for acetonitrile solutions of the complexes (5×10^{-4} M) in the presence of [$^nBu_4N$][PF_6] (0.1 M) as the supporting electrolyte by cyclic voltammetry (CV) at a scan rate of 100 $mV \cdot s^{-1}$ in a clockwise direction. Ferrocene was added at the end of all the experiments as the internal reference. The potential experimentally determined for the redox couple Fc^+/Fc was $E°_{1/2}$ = 0.455±0.002 V vs. Ag/AgCl. Therefore, the experimental redox potentials were calculated from the corresponding voltammograms as:

$E°$ (vs AgCl/Ag) = (E_{ap} + E_{cp})/2, for reversible peaks where E_{ap} and E_{cp} stand for anodic and cathodic peak potentials, respectively. However, for irreversible peaks, the potentials were calculated as either the E_{ap} maximum or E_{cp} minimum.

$E°$ (vs Fc^+/Fc) = $E°$ (vs AgCl/Ag) – 0.443, for potential values reported in reference to the (Fc^+/Fc) redox couple.

General protocol for the photooxidative thiocyanation of indoles

In a large test tube for catalysis (20 mL), 1.5 mmol of NH_4SCN, 0.5 mmol of indole (1470 μL from a stock solution of indole in THF 0.34 M) , 0.1 mol % of [**IrL2]** (681 μL from stock solution of **[IrL2]Cl** in THF 7.34×10^{-4} M) and 2849 μL of THF were added to to give a total volume of 5 mL and a final concentration of indole of 0.1 M. The tube was sealed with a septum and subsequently purged with a balloon of O_2 (1 atm, 10 min). The mixture was stirred for 24 h under blue light irradiation (LED strip, 5 m, λ_{ex} = 460 nm, 23 W, see experimental set-up in Figure S37). The yield values were determined by ^{1}H NMR of the crudes and are the averaged result of two independent experiments. 1,3,5-Trimethoxybenzene was used as internal reference for quantitative ^{1}H NMR determinations. For the isolated yields, the reaction mixture was diluted with dichloromethane (15 mL) and washed with brine. The combined organic phases were dried over $MgSO_4$**.** After removing the solvent under reduced pressure, the crude product was purified through silica gel column chromatography using a gradient of a mixture of petroleum ether/ethyl acetate (7:1 to 2:1). See ^{1}H NMR spectra of the reaction crude mixture in Figures S19-S26.

General protocol for the photodehydrogenation of indoline

In a test tube for catalysis (20 mL) equipped with a magnetic stirrer, 0.5 mmol of indoline (1470 μL from a stock solution of indole in THF 0.34 M) , 0.1 mol % of [**IrL2]** (681 μL from stock solution of **[IrL2]Cl** in THF 7.34×10^{-4} M) and 2849 μL of THF were added to give a total volume of 5 mL and a final concentration of indole of 0.1 M. The tubes were sealed with a septum and subsequently filled with a balloon of O_2 (1 atm, 10 min). The mixture was stirred for 24 h under blue light irradiation (LED strip, 5 m, λ_{ex} = 460 nm, 23 W, see experimental set-up in Figure S37). After 24 h the solvent was removed and the yield was estimated by ^{1}H NMR using 1,3,5 trimethoxybenzene as internal standard, as the averaged result of two independent experiments. See ^{1}H NMR spectra of the reaction crude mixture in Figures S27-S30. The ^{1}H NMR spectrum of **2a**, **2b**, **2d**, **2h**, **2l** and **2m** matches with those described in the bibliography.[7]

General protocol for the photocatalytic one-pot transformation of indolines into 3-thiocyanate indoles

In a test tube for catalysis (20 mL) equipped with a magnetic stirrer, 0.5 mmol of indoline (1470 μL from a stock solution of indole in THF 0.34 M) , 0.1 mol % of [**IrL2]** (681 μL from stock solution of **[IrL2]Cl** in THF 7.34×10^{-4} M) and 2849 μL of THF were added to complete 5 mL of volume and final concentration of indole of 0.1 M. The tube was sealed with a septum and subsequently filled with a balloon of O_2 (1 atm, 10 min). The mixture was stirred for 24 h under blue light irradiation (LED strip, 5 m, λ_{ex} = 460 nm, 23 W, see experimental set-up in Figure S37). After 24 h, 1.5 mmol of NH_4SCN was added. The tube was again sealed with a septum and filled with a balloon of O_2 (1 atm, 10 min). The mixture was stirred for other 24 h under blue light irradiation (λ_{exc}= 460 nm, 23 W). Then, the solvent was removed, and the yield was estimated by ^{1}H NMR using 1,3,5 trimethoxybenzene as internal standard. The yields were determined by averaging the result of two independent experiments. See ^{1}H NMR spectra of the reaction crude mixture in Figures S31-S34.

Gram-scale protocol for the one-pot transformation of 1a into 3a

In a 250 mL three-neck round-bottom flask, **1a** (1 g, 8.39 mmol) of indoline and 0.5 mol % of **[IrL2]Cl** were added and dissolved in THF (85 mL). The round bottom flask was sealed with a septum and subsequently filled with two balloons of O_2 (1 atm, 10 min). The mixture was stirred for 24 h under blue light irradiation (LED strip, 5 m, λ_{ex} = 460 nm, 23 W, see experimental set-up in Figure S38). After 24 h, 1.5 equiv. of NH_4SCN and filled with two balloons of O_2 (1 atm). The mixture was filled with another balloon of O_2 (1 atm) in the first 24 h and stirred again for 48 h under blue light irradiation (460 nm, 23 W). Finally, the product **3a** was purified by silica gel column chromatography using petroleum ether/ethyl acetate (5:1 – 2:1). Yield 71% (1.04 g, 5.96 mmol). See Figures S35 and S36.

2.- Synthesis and characterization of ligands L1-L3

Synthesis of 1-(thiazol-2-yl)-β -carboline (L1):

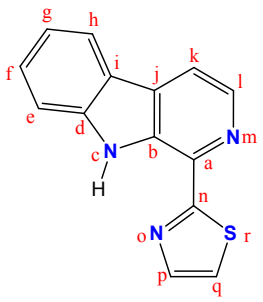

In a 100 mL Schlenk, tryptamine (200 mg, 1.22 mmol) and thiazol-2-carboxaldehyde (113 µL, 1.22 mmol) were heated at 155 °C in dry anisole (50 mL) for 3 h with continuous stirring. Then, activated MnO_2 (2.121 g, 20 equiv.) was added and the mixture was heated under reflux for an additional period of 21 h. The suspension was filtered while hot and the solvent was removed under vacuum to produce a yellow solid. 227 mg. Yield 74%. **^{1}H NMR (400 MHz, DMSO-d_6, 25 °C)** δ 11.67 (bs, 1H, NH), 8.43 (d, *J* = 5.1 Hz, 1H; H^l), 8.29 (d, *J* = 7.9 Hz, 1H; H^h), 8.26 (d, *J* = 5.8 Hz, 1H; H^k), 8.18 (d, *J* = 3.3 Hz, 1H; H^p), 7.94 (d, *J* = 3.2 Hz, 1H; H^q), 7.90 (d, *J* = 8.2 Hz, 1H; H^e), 7.59 (t, *J* = 8.3 Hz, 1H; H^f), 7.30 (t, *J* = 7.0 Hz, 1H; H^g) ppm. **^{13}C{^{1}H} NMR (101 MHz, DMSO-d_6, 25 °C)** δ 168.87, 144.18, 141.48, 138.00, 134.11, 131.35, 130.01, 128.64, 121.74, 121.64, 120.32, 119.95, 116.20, 113.25 ppm. **HRMS ESI(+)(DCM+DMSO) (*m/z*)** = $[M+H]^+$ calcd for $[C_{14}H_9N_3S]^+$ 252.0589; found 252,0593 Da. **Anal. Calcd (%) for $C_{14}H_9N_3S\cdot(H_2O)_1$:** C 62.44; H 4.12; N 15.60; S 11.91. **Found**: C 62.22; H 4.00; N 15.45; S 11.60.

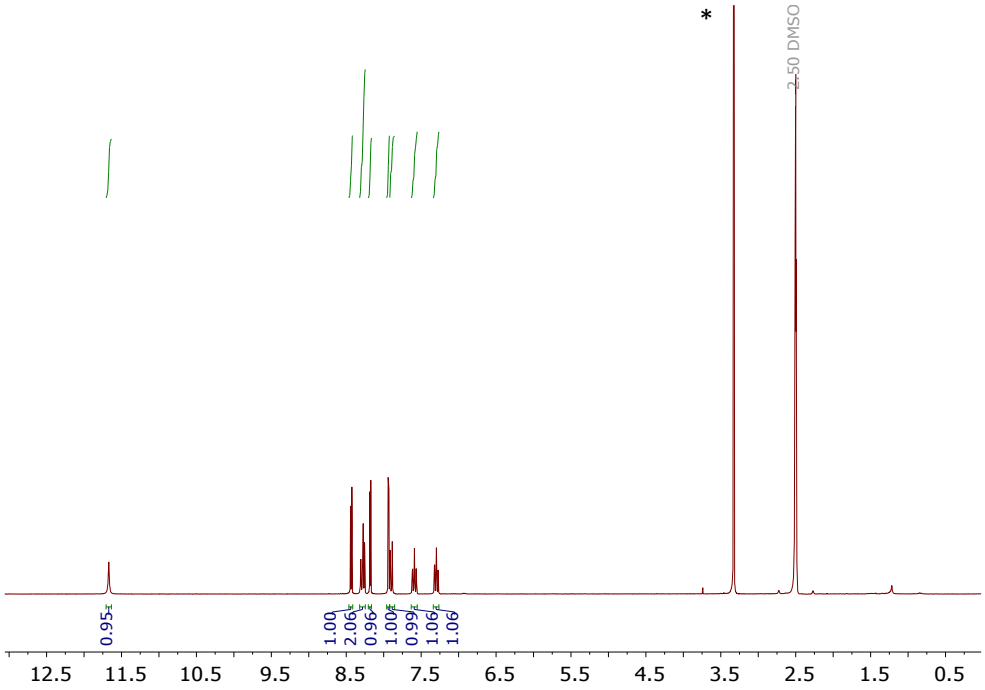

Figure S1. ^{1}H NMR (400 MHz, DMSO-d_6, 25 °C) spectrum of **L1** (* = H_2O).

Synthesis of 1-(5-methylthiazol-2-yl)-β-carboline (L2):

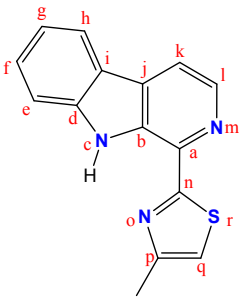

In a 100 mL Schlenk, tryptamine (0.215 g, 1.35mmol) and 4-methyl-2-thiazolecarboxaldehyde (145 µL, 1.35 mmol) were heated to 155 °C in dry anisole (50 mL) for 3 h with continuous stirring. Then, activated MnO_2 (2.347 g, 20 equiv.) was added and the mixture was heated under reflux for an additional period of 21 h. The suspension was filtered while hot and the solvent was removed under vacuum to produce a yellow solid. 0.198 g. Yield 55%. **^{1}H NMR (400 MHz, DMSO-d_6, 25 °C)** δ 11.43 (bs, 1H; NH), 8.40 (d, *J* = 5.0 Hz, 1H; H^l), 8.26 (d, *J* = 7.8 Hz, 1H; H^h), 8.20 (d, *J* = 5.0 Hz, 1H; H^k), 7.92 (d, *J* = 8.2 Hz, 1H; H^e), 7.59 (t, *J* = 7.7 Hz, 1H; H^f), 7.42 (s, 1H; H^q), 7.28 (t, *J* = 7.4 Hz, 1H; H^g), 2.62 (s, 3H; Me) ppm. **^{13}C{^{1}H} NMR (101 MHz, DMSO-d_6, 25 °C)** δ 167.81, 153.73, 141.30, 138.01, 134.17, 131.38, 129.89, 128.62, 121.71, 120.44, 119.92, 115.92, 115.87, 113.15, 17.16 (Me) ppm. **HRMS-ESI(+) *(m/z):*** $[M+H]^+$ calcd for $[C_{15}H_{12}N_3S]^+$ 266.0746; found, 266.0750. **Anal. Calc. (%) for $C_{15}H_{11}N_3S$:** C 67.9; H 4.18; N 15.84; S 12.08. **Found:** C 67.52; H 4.15; N 15.13; S 12.16.

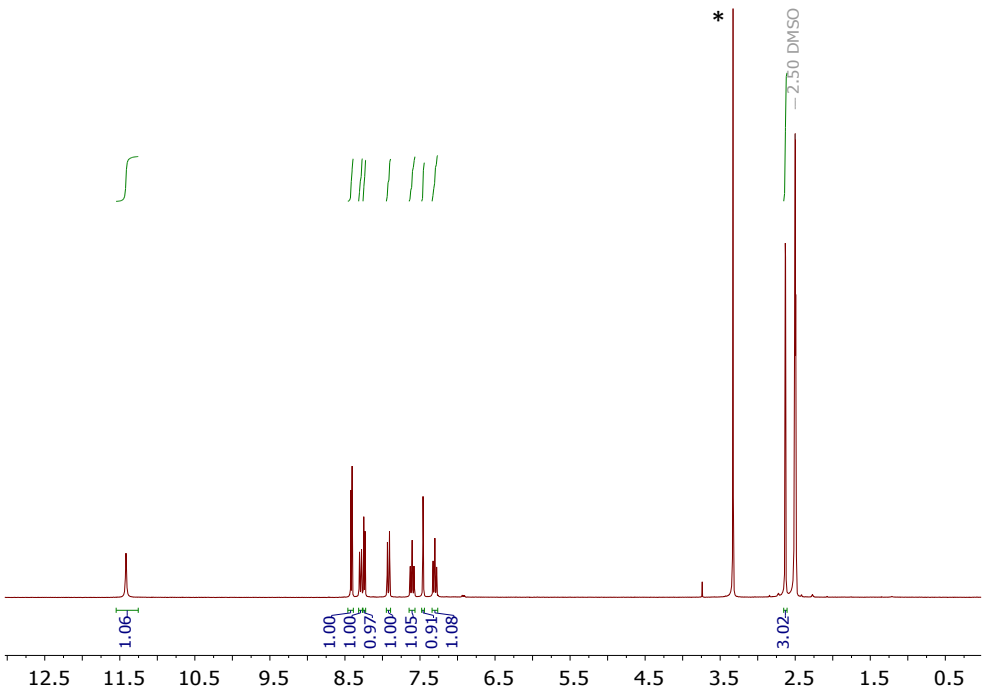

Figure S2. ^{1}H NMR (400 MHz, DMSO-d_6, 25 °C) spectrum of **L2** (* = H_2O).

Synthesis of 1-(benzothiazol-2-yl)-β-carboline (L3):

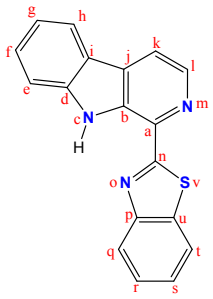

In a 100 mL Schlenk, tryptamine (0.215 g, 1.35 mmol) and benzothiazole-2-carboxaldehyde (0.216 g, 1.28 mmol) were heated to 155 °C in dry anisole (50 mL) for 21 h with continuous stirring. Then, activated MnO_2 (2.173g, 20 equiv.) was added to the mixture and refluxed for an additional period of 21 h. The suspension was filtered while hot and the solvent was removed under vacuum to produce a yellow solid. 0.089 g, Yield 59%. **^{1}H NMR (400 MHz, DMSO-d$_6$, 25 °C)** δ 11.78 (bs, 1H; NH), 8.54 (d, *J* = 5.1 Hz, 1H), 8.38 (d, *J* = 5.1 Hz, 1H; H^k), 8.35 (d, *J* = 8.0 Hz, 1H; H^h), 8.30 (d, *J* = 7.7 Hz, 1H; H^q), 8.22 (d, *J* = 8.0 Hz, 1H; H^t), 7.97 (d, *J* = 8.3 Hz, 1H; H^e), 7.68 – 7.62 (m, 2H; H^f, H^r), 7.54 (t, *J* = 8.2 Hz, 1H; H^s), 7.34 (t, , *J* = 8.0 Hz, 1H; H^g) ppm. **^{13}C{^{1}H} NMR (75 MHz, DMSO-*d*$_6$)** δ 154.07, 141.59, 138.40, 134.53, 133.57, 132.39, 130.33, 128.98, 126.60, 125.87, 123.20, 122.52, 121.95, 120.40, 120.24, 117.26, 113.28, 99.53 ppm. **HRMS-ESI(+) *(m/z):*** [M+H]$^+$ calcd for [$C_{18}H_{12}N_3S$]$^+$ 302.0746; found, 302.0753. **Anal. Calc. (%) for $C_{18}H_{11}N_3S$:** C 71.74; H 3.68; N 13.94; S 10.64. **Found:** C 71.35; H 3.43; N 13.01; S 11.81.

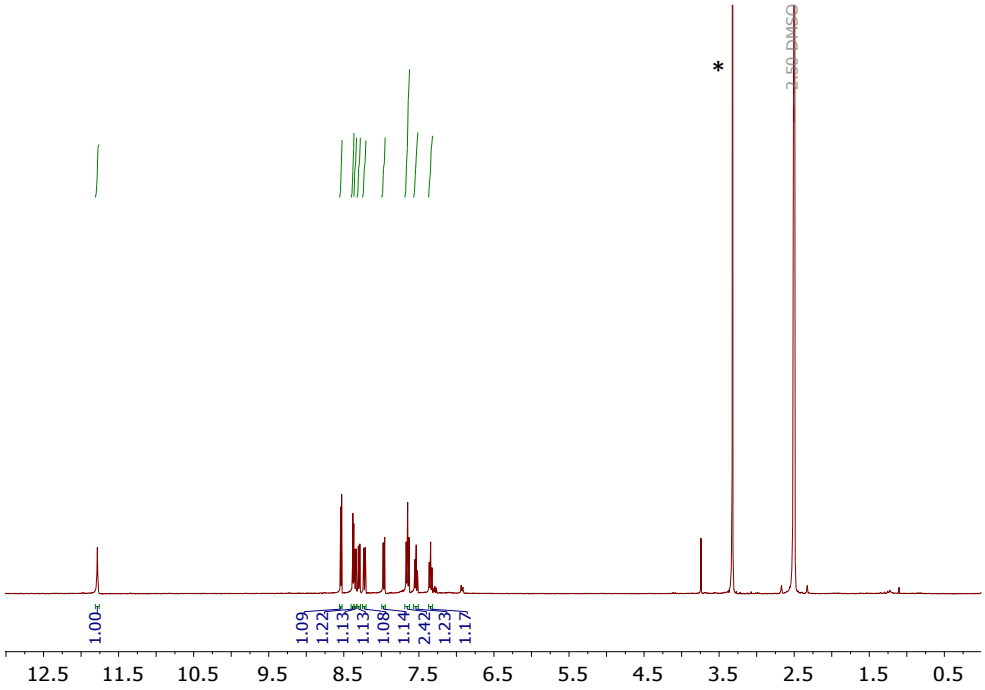

Figure S3. ^{1}H NMR (400 MHz, DMSO-*d*$_6$, 25 °C) spectrum of **L3** (* = H_2O).

3.- Synthesis and characterization of the complexes [IrL1]Cl–[Ir-L3]Cl

Synthesis of *rac*-[Ir(ppy)$_2$(L1)]Cl, ([IrL1]Cl):

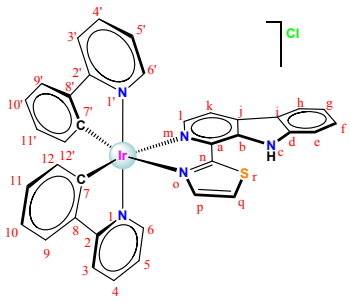

In a 100 mL Schlenk flask, previously purged with nitrogen, **L1** (0.05 g, 0.199 mmol) was added to a solution of [Ir(ppy)$_2$(μ-Cl)]$_2$ (0.100 g, 0.093 mmol) in a dichloromethane/methanol mixture (2:1, 25 mL). The mixture was stirred overnight at 50 °C under a nitrogen atmosphere. The solvent was removed under vacuum and the crude solid was washed with methyl tert-butyl ether (6 mL). Finally, the product was filtered, and dried under vacuum for 5 hours. Orange solid: 0.120 g. Yield 82%. **^{1}H NMR (400 MHz, DMSO-*d*$_6$, 25 °C)** δ 12.30 (bs, 1H; NH^c), 8.52 – 8.41 (m, 2H; H^p, H^l), 8.31 (d, *J* = 7.8 Hz, 1H; H^h), 8.29 – 8.22 (m, 2H; H^3, H$^{3'}$), 8.01 – 7.92 (m, 2H; H^4, H$^{4'}$), 7.92 – 7.84 (m, 3H; H^e, H^9, H$^{9'}$), 7.74 (t, *J* = 7.7 Hz, 1H; H^f), 7.67 (d, *J* = 5.7 Hz, 1H; H^k), 7.64 (d, *J* = 5.1 Hz, 1H; H$^{6 \text{ or } 6'}$), 7.57 (d, *J* = 5.4 Hz, 1H; H$^{6 \text{ or } 6'}$), 7.42 (t, *J* = 7.5 Hz, 1H; H^g), 7.26 (d, *J* = 3.3 Hz, 1H; H^q), 7.15 (t, *J* = 6.6 Hz, 1H; H$^{5 \text{ or } 5'}$), 7.08 – 6.98 (m, 3H; H^5 or H$^{5'}$, H^{10}, H$^{10'}$), 6.97 – 6.88 (m, 2H; H^{11}, H$^{11'}$), 6.26 (m, 2H; H^{12}, H$^{12'}$) ppm. **FT-IR (ATR) selected bands:** 3038 (υ, $\nu_{N\text{-}H}$), 1625, 1605, 1499, 1475, 1416, 1319, 1267, 1218, 1162, 1130, 1062, 1031, 752, 631, 562, 417. **HRMS-ESI(+) *(m/z):*** [M–Cl]$^+$ calcd for [$C_{36}H_{25}IrN_5S$]$^+$ 752.1459; found, 752.1418. **Anal. Cald. (%) for $C_{36}H_{25}ClIrN_5S\cdot(CH_2Cl_2)_1\cdot(Et_2O)_1$:** C 52.20; H 3.57; N 7.85; S 3.59. **Found**: C 52.14; H 3.52; N 7.53; S 2.73.

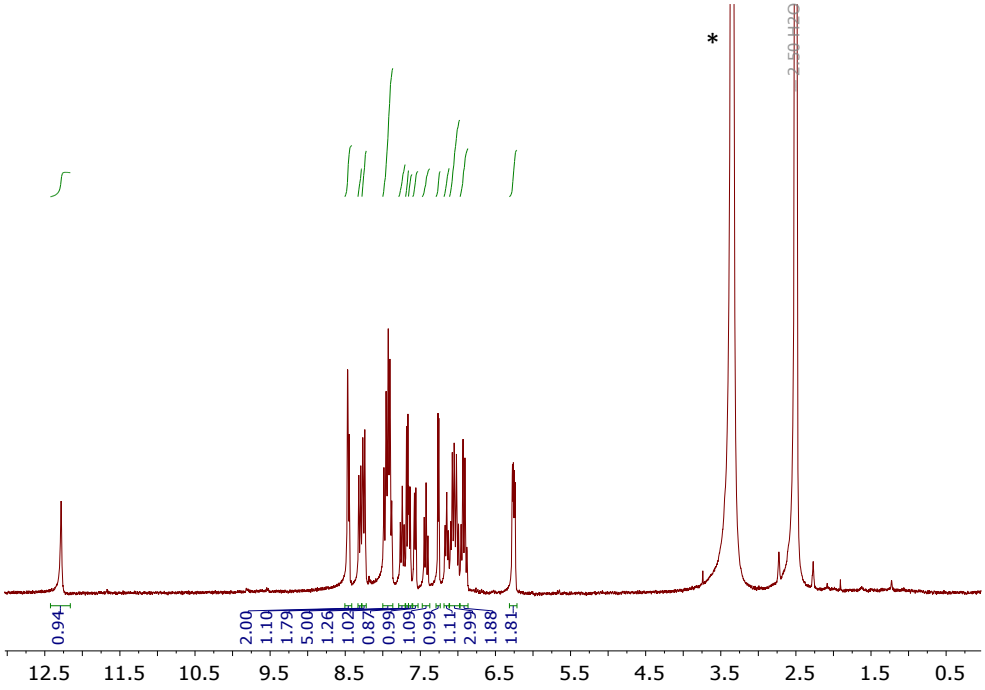

Figure S4. ^{1}H NMR (400 MHz, DMSO-*d*$_6$, 25 °C) spectrum of **[IrL1]Cl** (* = H_2O).

Synthesis of *rac*-[Ir(ppy)$_2$(L2)]Cl, ([IrL2]Cl):

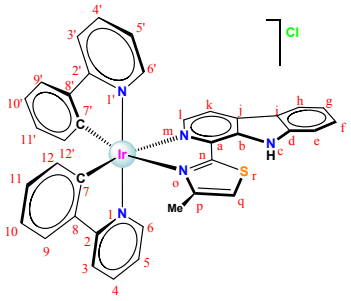

In a 100 mL Schlenk flask, previously purged with nitrogen, **L2** (0.054 g, 0.202 mmol) was added to a solution of [Ir(ppy)$_2$(μ-Cl)]$_2$ (0.100 g, 0.093 mmol) in a dichloromethane/methanol mixture (2:1, 25 mL). The mixture was stirred overnight at 50 °C under a nitrogen atmosphere. 30 mL of diethyl ether was added to precipitate the product and when the solid is completely formed, the solution was filtered under nitrogen. The solid was washed with additional 5 mL of diethyl ether under stirring (10 min.), filtered, and dried under vacuum for 5 hours. Orange solid. 0.111 g. Yield: 72%. **^{1}H NMR (400 MHz, DMSO-*d*$_6$, 25 °C)** δ 12.19 (bs, 1H; 1H; NH^c), 8.40 (d, *J* = 5.8 Hz, 1H; H^l), 8.29 – 8.25 (m, 3H; H^3, H$^{3'}$, H^h), 8.07 (s, 1H; H^q), 7.97 (d, *J* = 8.3 Hz, 1H; H^e), 7.94 – 7.89 (m, 4H; H^4, H$^{4'}$, H^9, H$^{9'}$), 7.83 (d, *J* = 5.9 Hz, 1H; H^6), 7.72 (t, *J* = 7.7 Hz, 1H; H^f), 7.56 (d, *J* = 5.7 Hz; 1H^k), 7.49 (d, *J* = 5.8 Hz, 1H; H$^{6'}$), 7.40 (t, *J* = 7.6 Hz, 1H; H^g), 7.19 (t, *J* = 6.6 Hz, 1H; H^5), 7.10 – 6.98 (m, 2H; H$^{10'}$, H$^{5'}$), 6.95 – 6.91 (m, 2H; H^{10}, H$^{11'}$), 6.82 (t, *J* = 7.4 Hz, 1H; H^{11}), 6.19 (d, *J* = 7.6 Hz, 1H; H^{12}), 6.10 (d, *J* = 7.5 Hz, 1H; H$^{12'}$), 1.74 (s, 3H; Me) ppm. **FT-IR (ATR) selected bands:** 3040 (υ, ν$_{N-H}$), 1604, 1581, 1500, 1475, 1419, 1315, 1267, 1223, 1161, 1132, 1063, 1031, 750, 556, 439. **HRMS-ESI(+) *(m/z):*** [M−Cl]$^+$ calcd for [C$_{37}$H$_{27}$IrN$_5$S]$^+$ 766.1616; found, 766.1616. **Anal. Calc. (%) for C$_{37}$H$_{27}$ClIrN$_5$S(H$_2$O)$_3$:** C 51.95; H 3.89; N 8.19; S 3.75. **Found:** C 51.96; H 3.55; N 7.94; S 3.00.

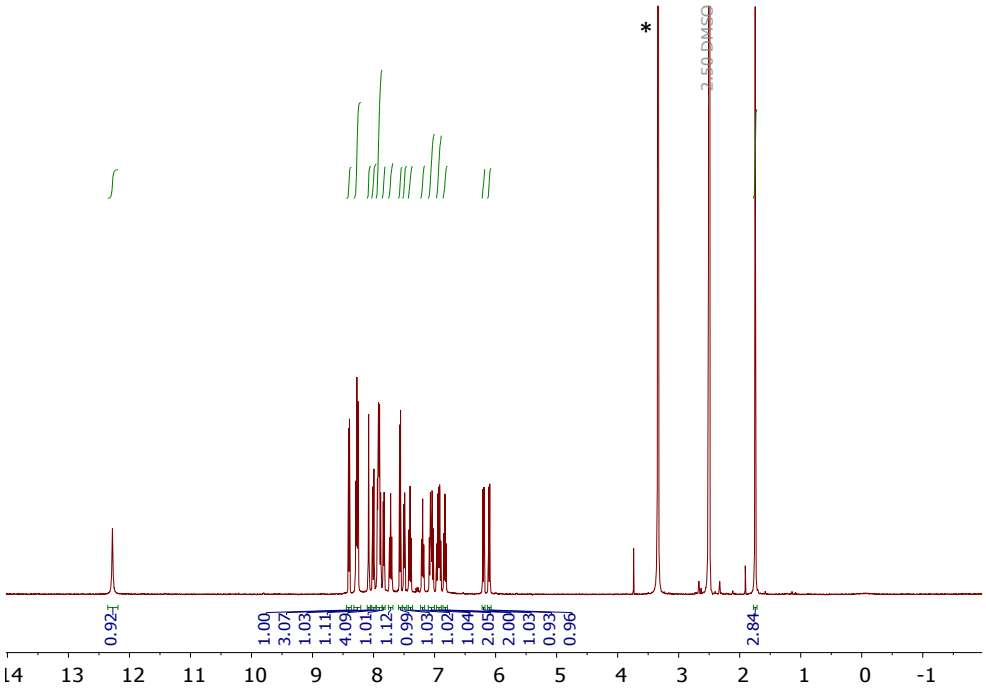

Figure S5. ^{1}H NMR (400 MHz, DMSO-*d*$_6$, 25 °C) spectrum of **[IrL2]Cl** (* = H$_2$O).

Synthesis of *rac*-[Ir(ppy)$_2$(L3)]Cl, ([IrL3]Cl):

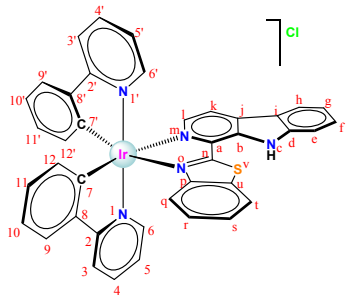

In a 100 mL Schlenk flask, previously purged with nitrogen, **L3** (0.054 g, 0.202 mmol) was added to a solution of [Ir(ppy)$_2$(μ-Cl)]$_2$ (0.116 g, 1.08 mmol) in a mixture dichloromethane/methanol (25 mL, 2:1). The mixture was stirred overnight at 50 °C under a nitrogen atmosphere. 30 mL of diethyl ether were added to precipitate the product and when the solid is completely formed, the ether was filtered under nitrogen. The solid was washed with additional 5 mL of Et_2O under stirring (10 min.), filtered, and dried under vacuum for 5 hours. Orange solid 0.102 g. Yield: 58%. **^{1}H NMR (400 MHz, DMSO-d$_6$, 25 °C)** δ 12.44 (s, 1H; NH^c), 8.53 (d, *J* = 5.7 Hz, 1H; H^l), 8.44 (d, *J* = 7.9 Hz, 1H; H$_{arom}$), 8.33 (d, *J* = 7.8 Hz, 1H; H^h), 8.28 (d, *J* = 8.0 Hz, 1H, H$_{arom}$), 8.21 (d, *J* = 8.0 Hz, 1H; H$_{arom}$), 8.03 (d, *J* = 8.3 Hz, 1H; H^e), 7.99 – 7.94 (m, 2H; 2H$_{arom}$), 7.93 – 7.91 (m, 1H; H$_{arom}$), 7.89 – 7.85 (m, 1H; H$_{arom}$), 7.82 (d, *J* = 5.9 Hz, 1H; H$_{arom}$), 7.77 (t, *J* = 8.3 Hz, 1H; H$_{arom}$), 7.71 (d, *J* = 5.7 Hz, 1H; H^k), 7.63 – 7.51 (m, 2H; H$^{9 \text{ or } 9'}$, H$_{arom}$), 7.44 (t, *J* = 7.5 Hz, 1H; H^g), 7.27 (t, *J* = 8.4 Hz, 1H; H$^{10 \text{ or } 10'}$), 7.14 – 7.06 (m, 3H; H$^{10 \text{ or } 10'}$, 2H$_{arom}$), 7.06 – 6.87 (m, 4H; H^{11}, H$^{11'}$, 2H$_{arom}$), 6.33 (d, *J* = 7.5 Hz, 1H; H$^{12 \text{ or } 12'}$), 6.16 (d, *J* = 7.5 Hz, 1H; H$^{12 \text{ or } 12'}$). **FT-IR (ATR) selected bands:** 3060 (υ, ν$_{N-H}$), 1605, 1581, 1498, 1476, 1455, 1417, 1323, 1268, 1211, 1160, 1126, 755, 680, 593, 418. **HRMS-ESI(+) *(m/z):*** [M–Cl]$^+$ calcd for [$C_{40}H_{27}IrN_5S$]$^+$ 802.1616; found, 802.1615. **Anal. Calc. (%) for $C_{40}H_{27}ClIrN_5S(H_2O)_{2.5}$:** C 54.44; H 3.66; N 7.94; S 3.63. **Found:** C 54.03; H 3.52; N 7.73; S 3.52.

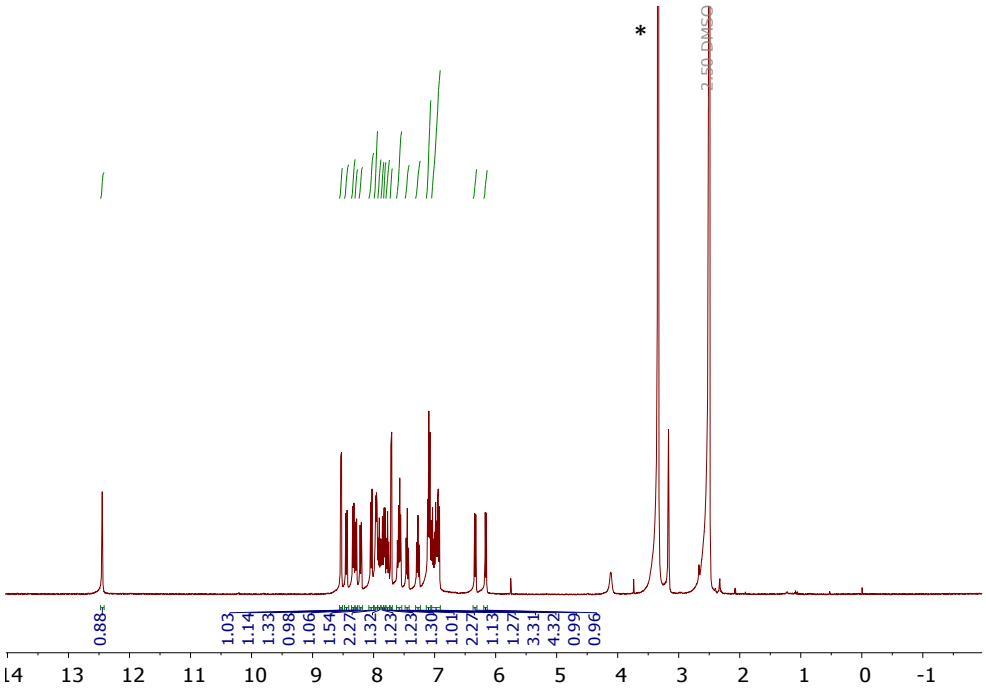

Figure S6. ^{1}H NMR (400 MHz, DMSO-*d*$_6$, 25 °C) spectrum of **[IrL3]Cl** (* = H_2O).

4.- X-Ray diffraction: Crystallographic parameters and spatial interactions

Table S1. Crystal data and structure refinement for **[IrL2]Cl·0.5CH_2Cl_2** and **[IrL3]Cl 0.5CH_3OH·0.75H_2O**		
Identification code	**[IrL2]Cl·0.5CH_2Cl_2**	**[IrL3]Cl·0.5CH_3OH·0.75H_2O**
Empirical formula	$C_{37.5}H_{28}Cl_2IrN_5S$	$C_{40.5}H_{30.5}ClIrN_5O_{1.25}S$
Formula weight	843.81	866.91
Temperature (K)	100(2)	100(2)
Wavelength (Å)	0.71073	1.54178
Crystal system	Monoclinic	Monoclinic
Space group	$P\,2_1/c$	$P\,2_1/n$
a(Å)	12.5200(11)	10.4860(6)
b(Å)	15.1527(12)	13.6234(7)
c(Å)	18.3721(15)	24.6492(13)
$\alpha(^o)$	90	90
$\beta(^o)$	101.752(3)	100.847(3)
$\gamma(^o)$	90	90
Volume(Å^3)	3412.3(5)	3458.3(3)
Z	4	4
Density (calculated) (g/cm^3)	1.642	1.665
Absorption coefficient (mm^{-1})	4.165	9.081
F(000)	1660	1714
Crystal size (mm^3)	0.10 x 0.10 x 0.05	0.08 x 0.05 x 0.05
Index ranges	-16 ≤ h≤ 16 -19 ≤ k ≤ 19 -23 ≤ l ≤ 22	-12 ≤ h ≤ 11 -16 ≤ k ≤ 16 -29 ≤ l ≤ 29
Reflections collected	61777	30708
Independent reflections	7859 [R(int) = 0.0679]	6111 [R(int) = 0.0755]
Data / restraints / parameters	7859 / 2 / 420	6111 / 597 / 493
Goodness-of-fit on F^2	1.089	1.061
Final R indices [$I>2\sigma(I)$]	0.0598, wR2 = 0.1354	0.0635, wR2 = 0.1553
Largest diff. peak / hole, e.Å^{-3}	5.192 / -2.911	2.311 / -1.792

Table S2. Hydrogen bonding parameters involving the NH group for **[IrL2]Cl·0.5CH_2Cl_2** and **[IrL3]Cl 0.5CH_3OH·0.75H_2O**.

Compound	**Interaction**	**dD---A (Å)**	**dH---A (Å)**	**dD-H (Å)**	**DHA (°)**	**Nature**
[IrL2]Cl·CH_2Cl_2	N3H3---Cl41 (NH---$ClCH_2Cl$)	3.03	2.39	0.88	130.1	Strong
[IrL3]Cl 0.5CH_3OH·0.75H_2O	N3H3A---Cl1 (NH---Cl^-)	3.20	2.44	0.88	144.6	Strong

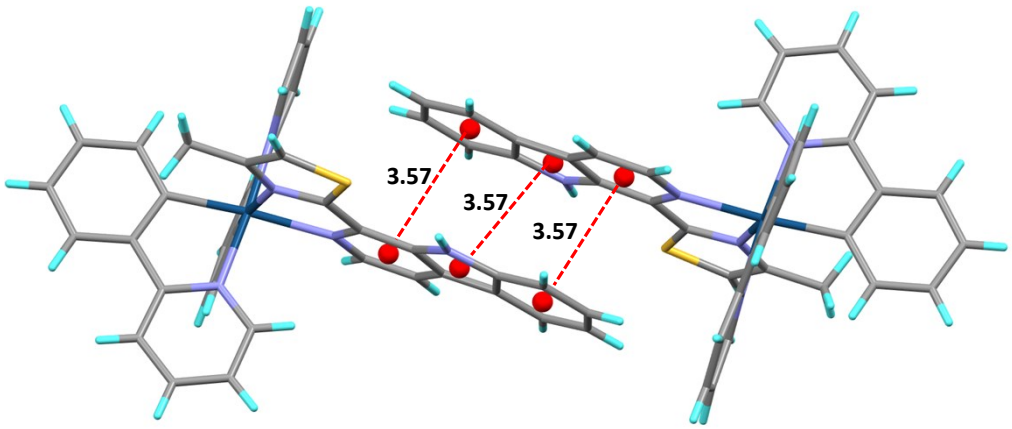

Figure S7. Complex **[IrL2]Cl**. Head-to tail π–π stacking interactions between the β-carboline ligands (distances between centroids in Å)

5.- Photostability of the [IrL1]Cl–[IrL3]Cl complexes

Photostability of the [IrL1]Cl–[IrL3]Cl complexes in CD_3CN

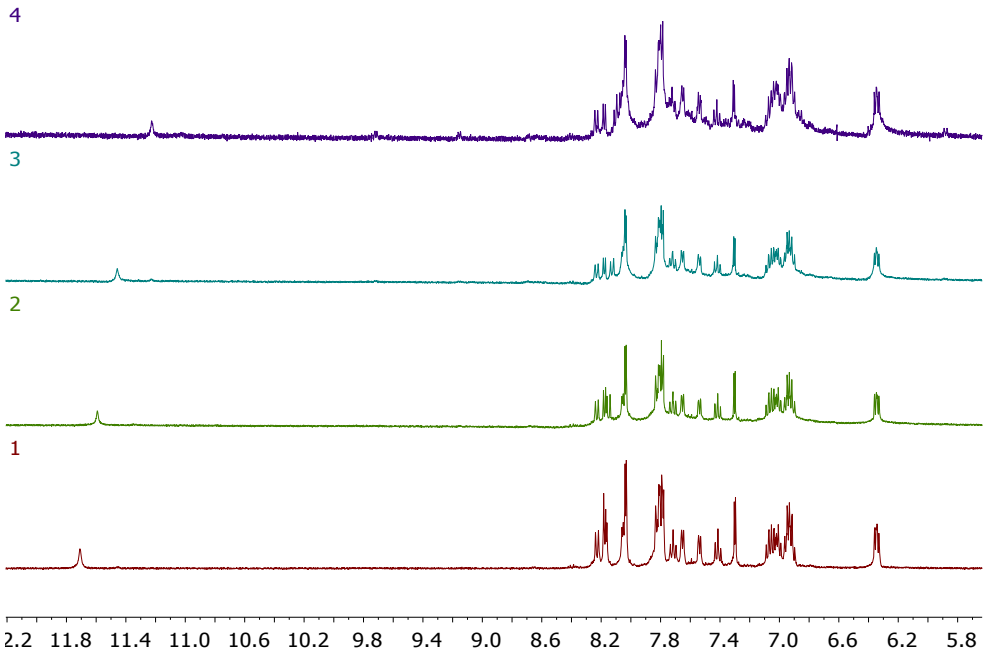

Figure S8. Evolution with time of the aromatic region of the ^{1}H NMR spectrum of **[IrL1]Cl** ($1.4\cdot10^{-2}$ M) in CD_3CN under irradiation (blue light, LED, λ = 460 nm, 24 W): 1) t = 0 , 2) t= 2 h, 3) t = 6h, 4) t = 24 h.

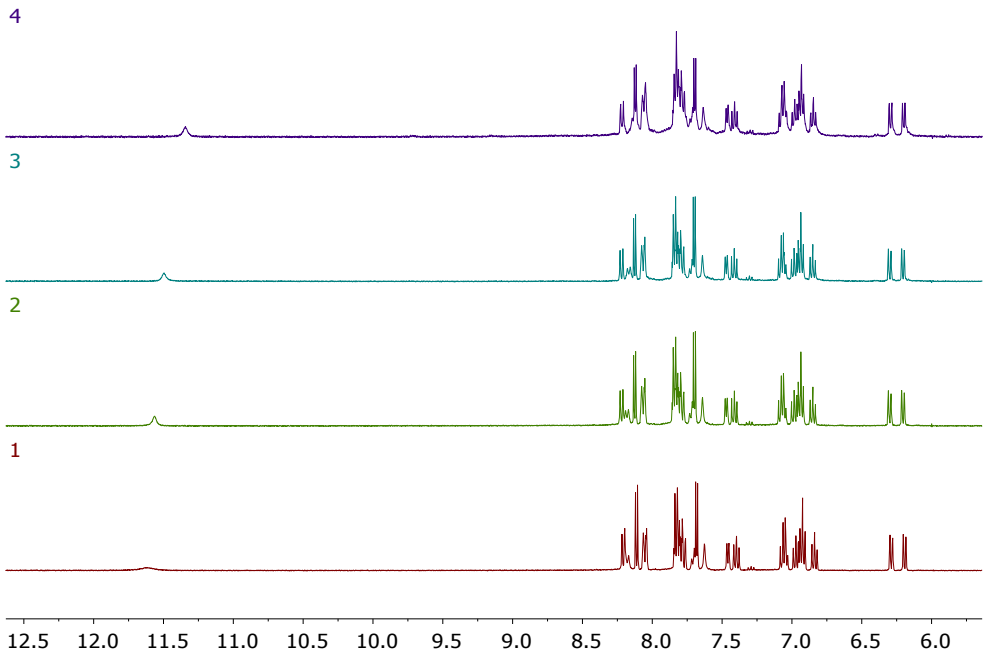

Figure S9. Evolution with time of the aromatic area of the ^{1}H NMR spectra of **[IrL2]Cl** ($1.4 \cdot 10^{-2}$ M) in CD_3CN under irradiation (blue light, LED, λ = 460 nm, 24 W): 1) t = 0 , 2) t= 2 h, 3) t = 6h, 4) t = 24 h.

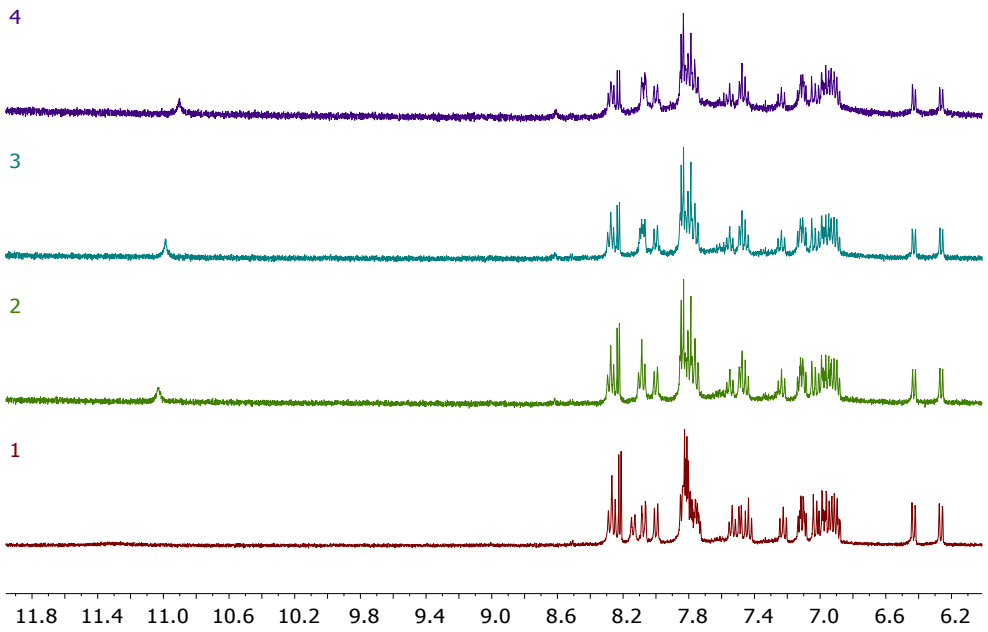

Figure S10. Evolution with time of the aromatic area of the ^{1}H NMR spectra of **[IrL3]Cl** ($1.4 \cdot 10^{-2}$ M) in CD_3CN under irradiation (blue light, LED, λ = 460 nm, 24 W): 1) t = 0 , 2) t= 2 h, 3) t = 6h, 4) t = 24 h.

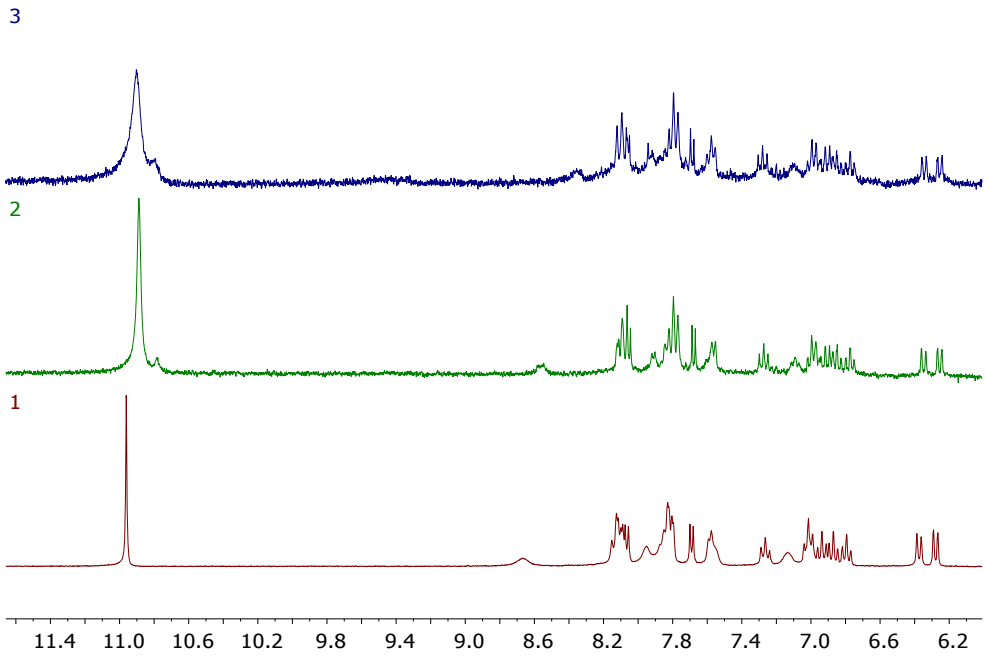

Figure S11. Aromatic area of the ^{1}H NMR spectra of **[IrL2]Cl** ($1.4 \cdot 10^{-2}$ M) in THF-d_6 under irradiation (blue light, LED, λ = 460 nm, 24 W): 1) t = 0 , 2) t= 6 h, 3) t = 24 h.

6.- Theoretical calculations.

Density functional theory (DFT) and time-dependent DFT (TD-DFT) calculations were carried out using the functional B3LYP[8,9] adding the atom-pairwise dispersion correction with the Becke-Johnson damping scheme (D3BJ)[10,11]. Double-Z basis set 6-31G(d,p)[12] were used to define all the elements but Ir that was defined with LANL2DZ basis.[13] The continuum solvation model SMD was used to take into account solvent effects.[14] All calculations were performed using the ORCA 4.2.0 package.[15,16]

Table S3. Topology of the molecular orbitals for **[1]**$^{+}$ and **[IrL1]**$^{+}$**–[IrL3]**$^{+}$

	[1]$^{+}$	**[IrL1]**$^{+}$	**[IrL2]**$^{+}$	**[IrL3]**$^{+}$

LUMO +3	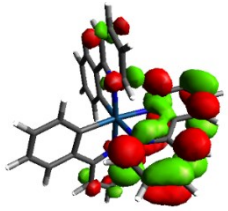 -1.253	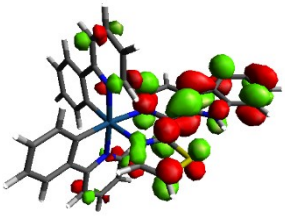 -1.135	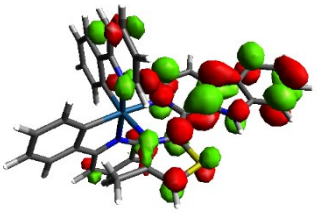 -1.095	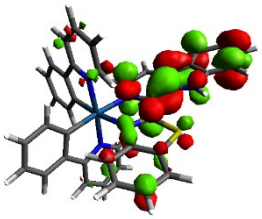 -1.164
LUMO +2	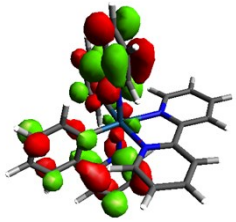 -1.420	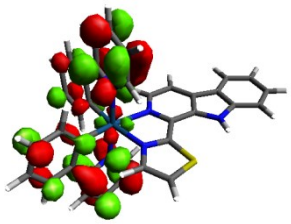 -1.418	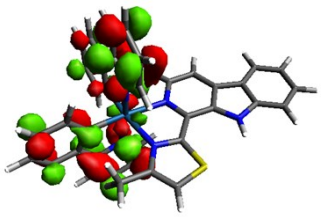 -1.412	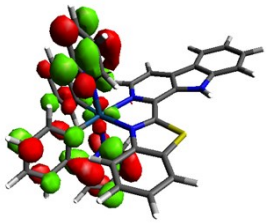 -1.431
LUMO +1	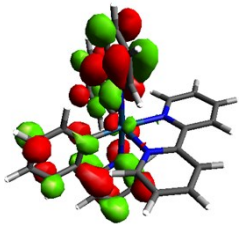 -1.506	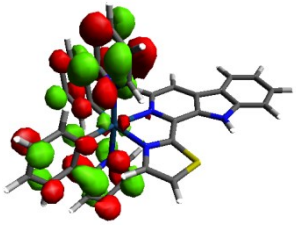 -1.509	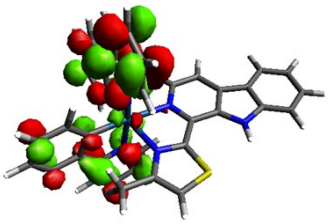 -1.525	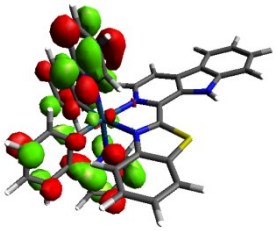 -1.536
LUMO	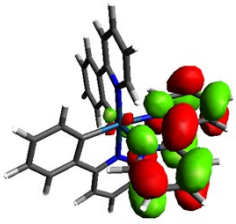 -2.104	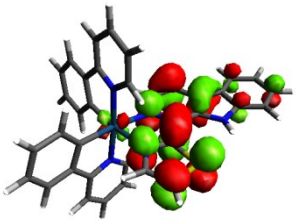 -2.438	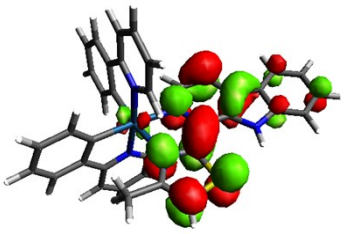 -2.405	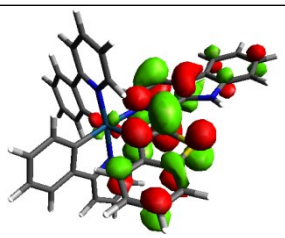 -2.555
HOMO	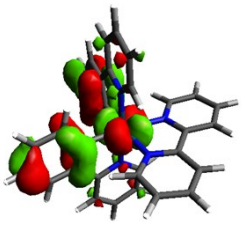 -5.422	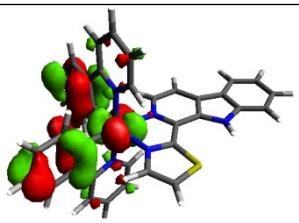 -5.422	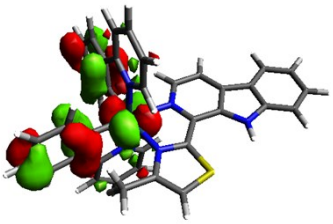 -5.448	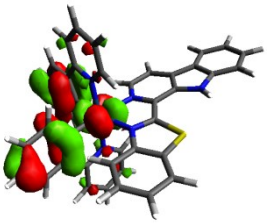 -5.5468

HOMO -1	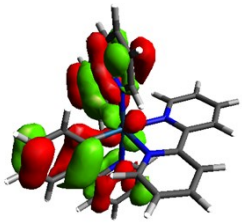 -6.065	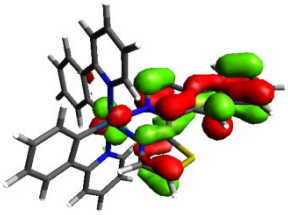 -5.976	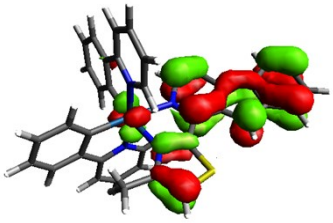 -5.955	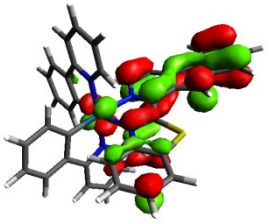 -5.987
HOMO -2	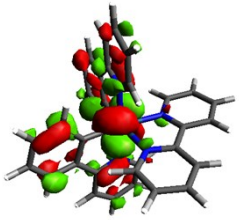 -6.182	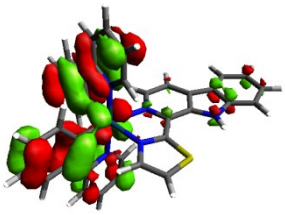 -6.066	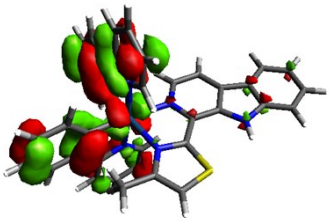 -6.047	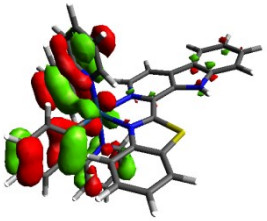 -6.073
HOMO -3	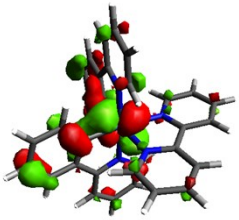 -6.299	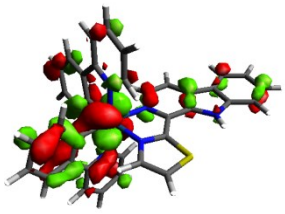 -6.169	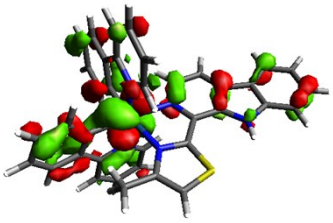 -6.137	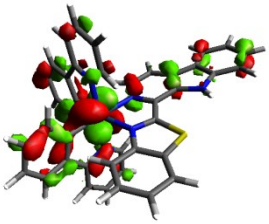 -6.169
HOMO -4		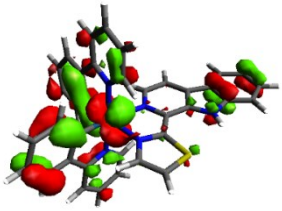 6.282	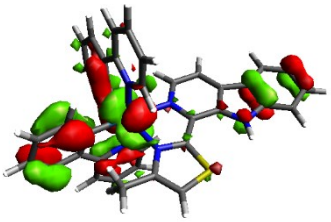 -6.270	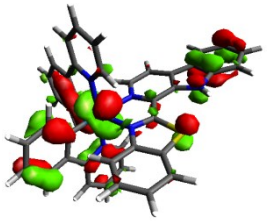 -6.282

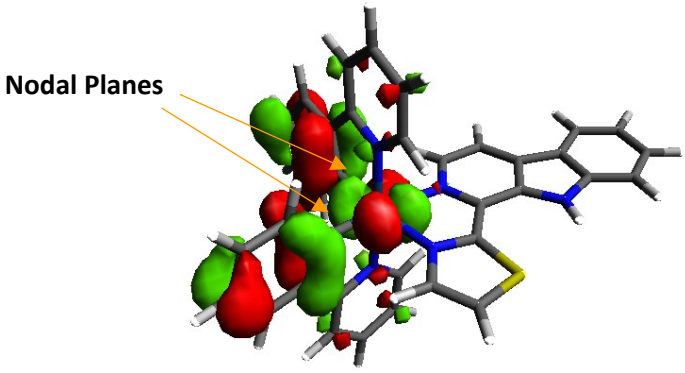

Figure S12. HOMO for **[IrL1]**$^{+}$, showing the two nodal planes at the Ir-C_{phenyl} interfaces.

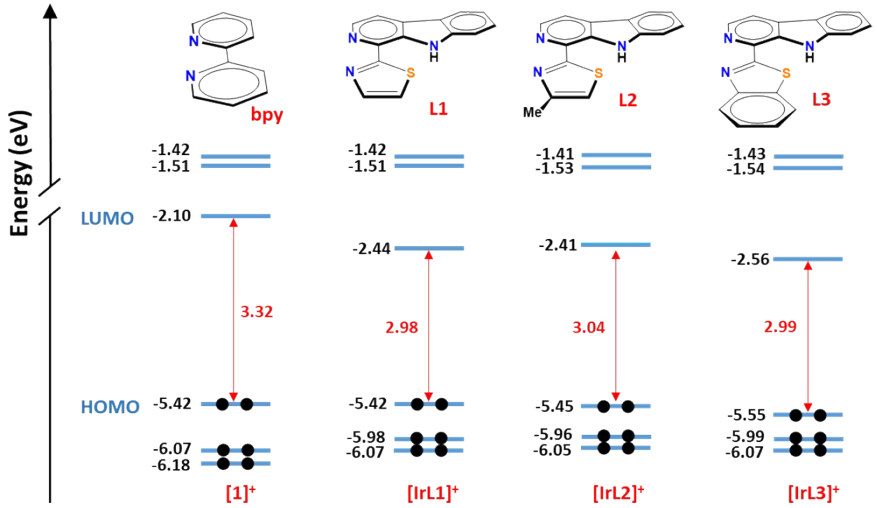

Figure S13. Schematic representation showing the energies calculated for the frontier molecular orbitals and the HOMO-LUMO energy gaps of **[1]**$^{+}$ and **[IrL1]**$^{+}$–**[IrL3]**$^{+}$.

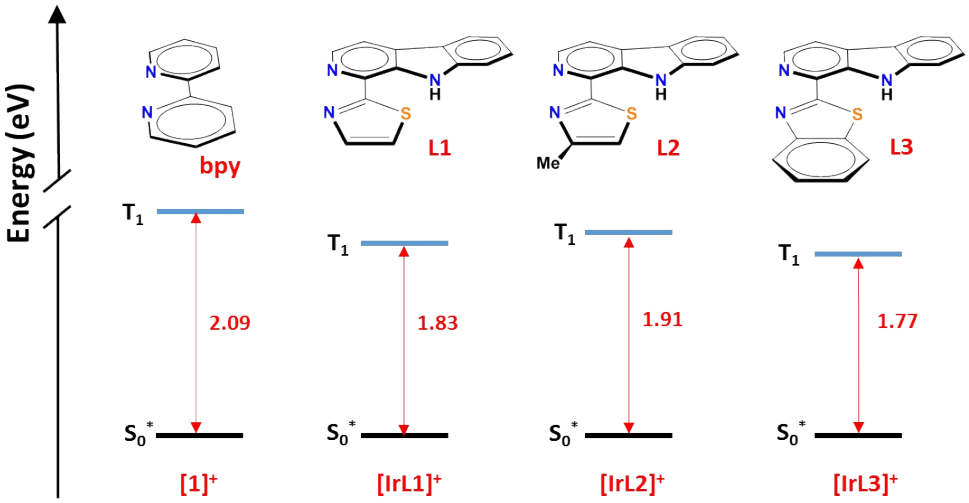

Figure S14. Energy diagram showing the calculated energy difference values between the lowest triplet excited state (T_1) and the singlet state keeping the geometry of the respective triplet (S_0*) for complexes **[IrL1]**$^{+}$–**[IrL3]**$^{+}$ and **[1]**$^{2+}$.

Table S4: Lowest triplet excited states calculated at the TD-DFT B3LYP/(6-31G**+LANL2DZ) level for complexes **[1]**$^{+}$ and **[IrL1]**$^{+}$ to **[IrL3]**$^{+}$ in acetonitrile solution.[a]

Complex	State	Energy (eV)	λ (nm)	f	Monoexcitations	Nature[b]	Description[c]
[1]$^{+}$	T_1	1.717	722.10		HOMO → LUMO (100)	$d_\pi(Ir) + \pi_{ppy} \rightarrow \pi^*_{bpy}$	^{3}MLCT /^{3}LLCT
	T_2	2.819	439.82		HOMO → LUMO+1 (85)	$d_\pi(Ir) + \pi_{ppy} \rightarrow \pi^*_{ppy}$	^{3}MLCT /^{3}LC
	T_3	2.880	430.50		HOMO-1 → LUMO+1 (19)	$d_\pi(Ir) + \pi_{ppy} \rightarrow \pi^*_{ppy}$	^{3}MLCT /^{3}LC
					HOMO → LUMO+2 (78)	$d_\pi(Ir) + \pi_{ppy} \rightarrow \pi^*_{ppy}$	^{3}MLCT /^{3}LC
	S_1	2.220	558.49	0.0002	HOMO → LUMO (100)	$d_\pi(Ir) + \pi_{ppy} \rightarrow \pi^*_{bpy}$	^{1}MLCT /^{1}LLCT
	S_2	3.024	410.00	0.0001	HOMO-2 → LUMO (92)	$d_\pi(Ir) + \pi_{ppy} \rightarrow \pi^*_{bpy}$	^{1}MLCT /^{1}LLCT
	S_3	3.138	395.11	0.0505	HOMO → LUMO+1 (99)	$d_\pi(Ir) + \pi_{ppy} \rightarrow \pi^*_{ppy}$	^{1}MLCT /^{1}LC

[IrL1]$^+$	T_1	1.541	804.57		HOMO → LUMO (96)	$d_\pi(Ir) + \pi_{ppy} \rightarrow \pi^*_{N^N}$	^{3}MLCT /^{3}LLCT
	T_2	2.394	517.90		HOMO-1 → LUMO (86)	$d_\pi(Ir) + \pi_{N^N} \rightarrow \pi^*_{N^N}$	^{3}MLCT /^{3}LC
	T_3	2.546	486.98		HOMO-3 → LUMO (48) HOMO-2 → LUMO (37)	$d_\pi(Ir) + \pi_{ppy} \rightarrow \pi^*_{N^N}$ $d_\pi(Ir) + \pi_{ppy} \rightarrow \pi^*_{N^N}$	^{3}MLCT /^{3}LLCT ^{3}MLCT /^{3}LLCT
	S_1	1.933	641.41	0.0001	HOMO → LUMO (100)	$d_\pi(Ir) + \pi_{ppy} \rightarrow \pi^*_{N^N}$	^{1}MLCT /^{1}LLCT
	S_2	2.783	445.51	0.0101	HOMO-3 → LUMO (47) HOMO-2 → LUMO (16) HOMO-1 → LUMO (26)	$d_\pi(Ir) + \pi_{ppy} \rightarrow \pi^*_{N^N}$ $d_\pi(Ir) + \pi_{ppy} \rightarrow \pi^*_{N^N}$ $d_\pi(Ir) + \pi_{N^N} \rightarrow \pi^*_{N^N}$	^{1}MLCT /^{1}LLCT ^{1}MLCT /^{1}LLCT ^{1}MLCT /^{1}LC
	S_3	2.816	440.28	0.1204	HOMO-3 → LUMO (63) HOMO-2 → LUMO (35)	$d_\pi(Ir) + \pi_{ppy} \rightarrow \pi^*_{N^N}$ $d_\pi(Ir) + \pi_{ppy} \rightarrow \pi^*_{N^N}$	^{1}MLCT /^{1}LLCT ^{1}MLCT /^{1}LLCT
[IrL2]$^+$	T_1	1.728	717.50		HOMO → LUMO (89)	$d_\pi(Ir) + \pi_{ppy} \rightarrow \pi^*_{N^N}$	^{3}MLCT /^{3}LLCT
	T_2	2.396	517.46		HOMO-1 → LUMO (80)	$d_\pi(Ir) + \pi_{N^N} \rightarrow \pi^*_{N^N}$	^{3}MLCT / ^{3}LC
	T_3	2.570	482.43		HOMO-3 → LUMO (59)	$d_\pi(Ir) + \pi_{ppy} \rightarrow \pi^*_{N^N}$	^{3}MLCT /^{3}LLCT
					HOMO-2 → LUMO (27)	$d_\pi(Ir) + \pi_{ppy} \rightarrow \pi^*_{N^N}$	^{3}MLCT /^{3}LLCT
	S_1	1.995	621.47	0.0001	HOMO → LUMO (100)	$d_\pi(Ir) + \pi_{ppy} \rightarrow \pi^*_{N^N}$	^{1}MLCT /^{1}LLCT
	S_2	2.786	445.03	0.0889	HOMO-2→ LUMO (71)	$d_\pi(Ir) + \pi_{ppy} \rightarrow \pi^*_{N^N}$	^{1}MLCT /^{1}LLCT
					HOMO-1 → LUMO (29)	$\pi_{N^N} \rightarrow \pi^*_{N^N}$	^{1}LC
	S_3	2.787	444.87	0.0101	HOMO-3 → LUMO (47)	$d_\pi(Ir) + \pi_{ppy} \rightarrow \pi^*_{N^N}$	^{1}MLCT /^{1}LLCT
					HOMO-1 → LUMO (27)	$\pi_{N^N} \rightarrow \pi^*_{N^N}$	^{1}LC
[IrL3]$^+$	T_1	1.514	818.92		HOMO → LUMO (97)	$d_\pi(Ir) + \pi_{ppy} \rightarrow \pi^*_{N^N}$	^{3}MLCT /^{3}LLCT
	T_2	2.330	532.12		HOMO-1 → LUMO (91)	$d_\pi(Ir) + \pi_{N^N} \rightarrow \pi^*_{N^N}$	^{3}MLCT /^{3}LC
	T_3	2.461	503.80		HOMO-3 → LUMO (59) HOMO-2 → LUMO (29)	$d_\pi(Ir) + \pi_{ppy} \rightarrow \pi^*_{N^N}$ $d_\pi(Ir) + \pi_{ppy} \rightarrow \pi^*_{N^N}$	^{3}MLCT /^{3}LLCT ^{3}MLCT /^{3}LLCT
	S_1	1.890	656.00	0.0001	HOMO → LUMO (100)	$d_\pi(Ir) + \pi_{ppy} \rightarrow \pi^*_{N^N}$	^{1}MLCT /^{1}LLCT
	S_2	2.654	467.16	0.0843	HOMO-2 → LUMO (76) HOMO-1 → LUMO (24)	$d_\pi(Ir) + \pi_{ppy} \rightarrow \pi^*_{N^N}$ $d_\pi(Ir) + \pi_{N^N} \rightarrow \pi^*_{N^N}$	^{1}MLCT /^{1}LLCT ^{1}MLCT /^{1}LC
	S_3	2.686	461.59		HOMO-3 → LUMO (50) HOMO-1 → LUMO (25)	$d_\pi(Ir) + \pi_{N^N} \rightarrow \pi^*_{N^N}$ $d_\pi(Ir) + \pi_{ppy} \rightarrow \pi^*_{N^N}$	^{1}MLCT /^{1}LC ^{1}MLCT /^{1}LLCT

[a] Vertical excitation energies (E), dominant monoexcitations with contributions (within parentheses) greater than 15%, nature of the electronic transition and description of the excited state are summarized. H and L denote HOMO and LUMO, respectively. [b]ppy = phenylpyridine ligand. (N^N:) = bidentate nitrogen donor ligand. [c]LC, MLCT, and LLCT denote ligand-centered, metal-to-ligand charge transfer, and ligand-to-ligand charge transfer,respectively.

Table S5. Participation of the atomic orbitals of the metal and the three ligands in the molecular orbitals.

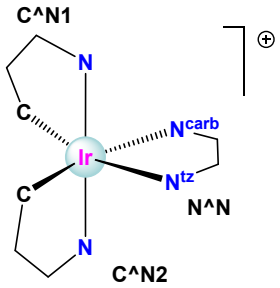

		HOMO-3	HOMO-2	HOMO-1	HOMO	LUMO	LUMO+1	LUMO+2
[1]$^+$	**Ir**	57,32	62,75	16,10	47,53	3,90	4,92	5,65
	C^N1	17,51	16,01	40,56	24,39	1,25	46,43	45,20
	C^N2	17,39	16,17	40,55	24,40	1,25	45,49	45,96
	N^N	7,78	5,07	2,78	3,68	93,60	3,17	3,20
[IrL1]$^+$	**Ir**	49,14	21,88	13,29	47,13	3,83	4,81	5,55
	C^N1	14,30	34,57	3,17	24,33	1,06	48,91	42,73
	C^N2	20,54	31,43	2,70	24,29	1,14	42,88	49,27
	N^N	16,01	12,12	80,84	4,25	93,98	3,40	2,45
[IrL2]$^+$	**Ir**	50,75	17,88	10,72	47,70	3,84	4,82	5,80
	C^N1	14,63	38,74	3,17	21,72	1,15	54,49	37,32
	C^N2	16,96	33,15	3,37	26,77	1,10	37,19	54,33
	N^N	17,66	10,22	82,73	3,81	93,91	3,50	2,56
[IrL3]$^+$	**Ir**	52,28	16,08	14,73	47,50	3,69	4,81	5,79
	C^N1	14,88	38,88	3,26	22,98	1,10	48,30	42,97
	C^N2	16,71	35,02	2,27	25,51	1,01	42,64	48,03
	N^N	16,12	10,01	79,74	4,00	94,20	4,24	3,21

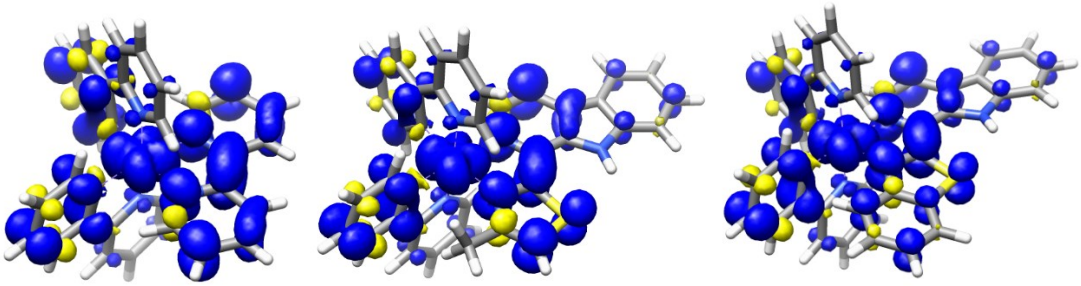

Figure S15. Unpaired-electron spin-density contours (0.002 au) calculated for the fully relaxed T_1 state of complexes **[1]$^+$**, **[IrL2]$^+$** and **[IrL3]$^+$**.

7.-Cyclic Voltammograms and electrochemical data of [IrL1]Cl–[IrL3]Cl.

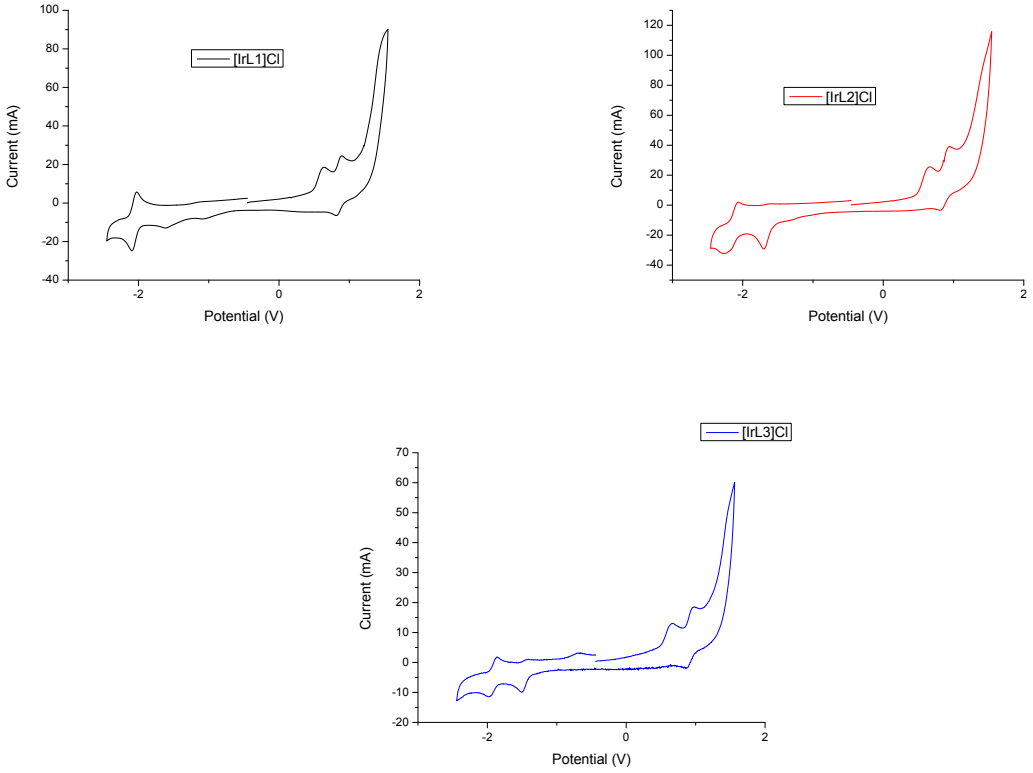

Figure S16. Cyclic voltammograms **[IrL1]Cl**–**[IrL3]Cl**.

8.- Photocatalytic Thiocyanation experiments and ^{1}H NMR spectra of the isolated products 3a-3h

Table S6. Photocatalytic thiocyanation of 1*H*-indole (**2a**) in the presence of RB and **[IrL1]Cl** at different times.

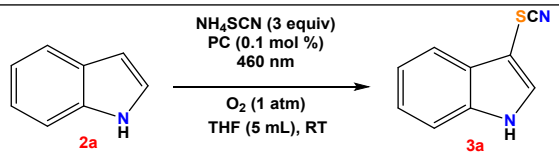

Entry	PC	Time (h)	Yield (%)
1	**RB**	24	97
2	**RB**	20	96
3	**RB**	6	46
4	**[1]Cl**	24	75
5	**[1]Cl**	20	63
6	**[1]Cl**	6	33

[a]General reaction conditions: 1*H*-indole (**2a**, 0.5 mmol), NH_4SCN (1.5 mmol, 3 equiv), catalyst (0.1 mol %), THF (5 mL), balloon of pure O_2 (1 atm, 10 min), under blue light (LED, λ_{irr} = 460 nm, 23 W), at room temperature for the specified time. The yield values were determined by ^{1}H NMR of the crudes and are the averaged result of two

independent experiments. 1,3,5-Trimethoxybenzene was used as internal reference for quantitative ^{1}H NMR determinations.

NMR characterization of isolated products[17]

3-Thiocyanato-1H-indole (3a):

Reaction: Indole **2a** (58.6 mg, 0.5 mmol), NH_4SCN (114 mg, 1.5 mmol), **[IrL2]Cl** (0.1 mol %), THF 5 mL, 24 h. Pale brown solid (84.5 mg, Isolated Yield: 97%). **^{1}H NMR (300 MHz, $CDCl_3$, 25 °C):** δ 8.62 (s, 1H), 7.84-7.79 (m, 1H), 7.56 (d, *J* = 2.8 Hz, 1H), 7.49-7.42 (m, 1H), 7.37 – 7.30 (m, 1H) ppm. **MS EI(+) (CH_2Cl_2)**: m/z = 174.0 (174.0 calcd. for $[C_9H_6N_2S]^+$).

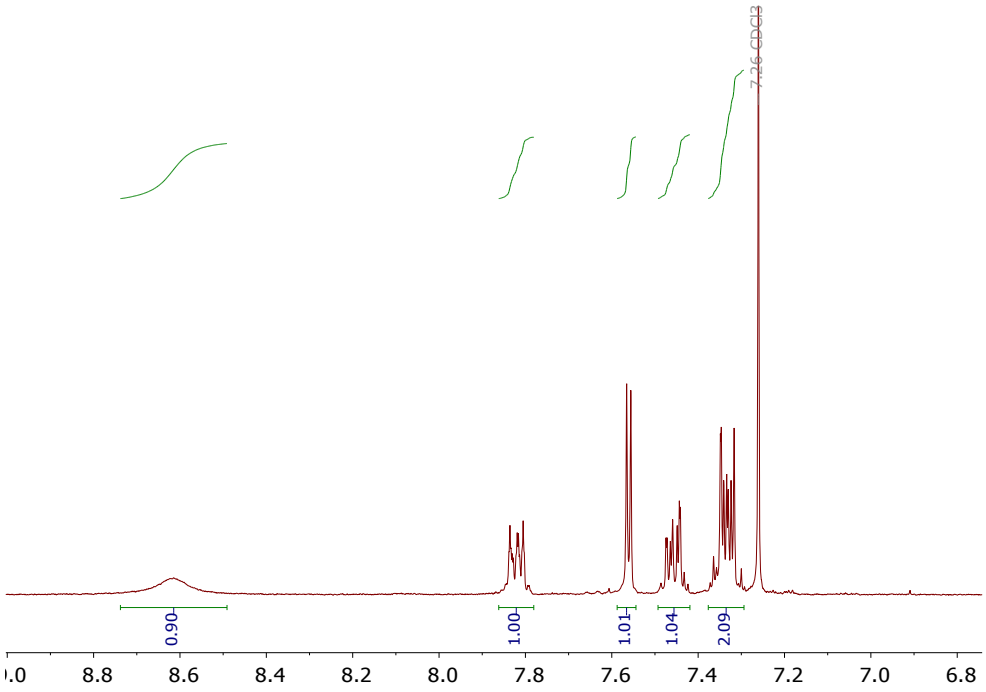

Figure S17. Aromatic area of the ^{1}H NMR (300 MHz, $CDCl_3$, 25 °C) spectrum of isolated **3a**.

5-fluoro-3-thiocyanato-1H-indole (3b):

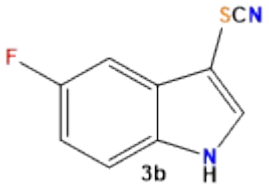

Reaction: 5-Fluoro-1*H*-indole **2b** (67.6 mg, 0.5 mmol), NH_4SCN (114 mg, 1.5 mmol), **[IrL2]Cl** (0.1 mol %), THF 5 mL, 24 h**.** White solid (87.4 mg, Isolated Yield: 91%). **^{1}H NMR (300 MHz, $CDCl_3$, 25 °C):** δ 8.64 (s, 1H), 7.59 (d, *J* = 2.9 Hz, 1H), 7.46 (dd, *J* = 8.8, 2.5 Hz, 1H), 7.38 (dd, *J* = 8.9, 4.1 Hz, 1H), 7.08 (td, *J* = 9.0, 2.5 Hz, 1H) ppm. **LMS EI(+) (CH_2Cl_2)**: m/z = 191.8 (192.2 calcd. for $[C_9H_5FN_2S]^+$).

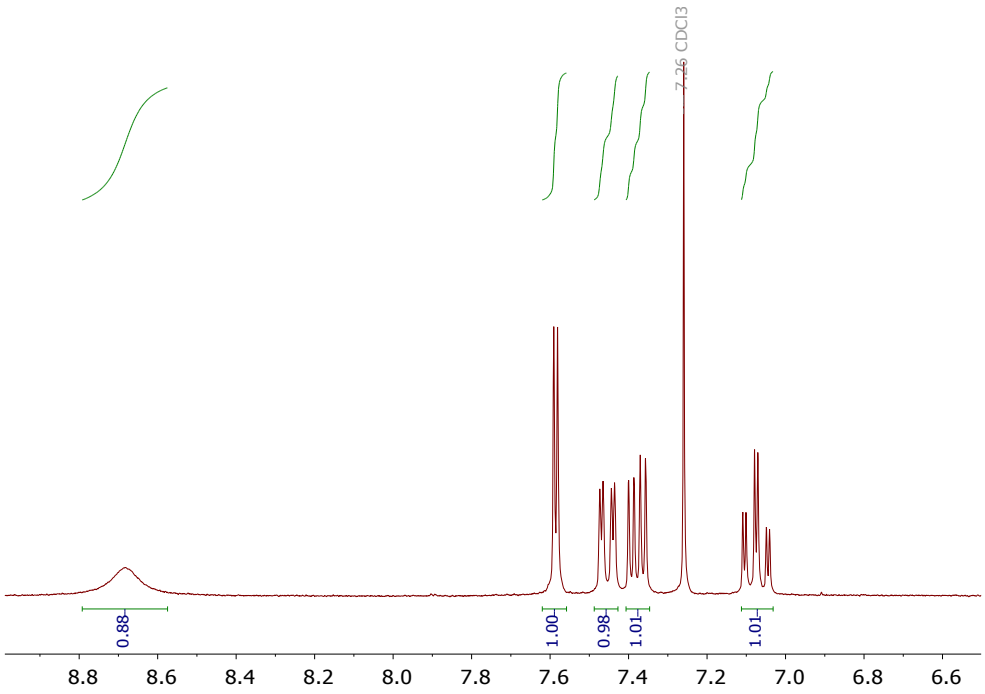

Figure S18. Aromatic area of the ^{1}H NMR (300 MHz, $CDCl_3$, 25 °C) spectrum of isolated **3b**.

5-chloro-3-thiocyanato-1H-indole (3c):

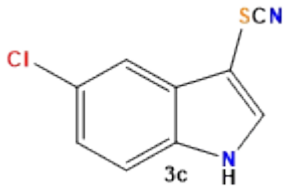

Reaction: 5-Chloro-1*H*-indole **2c** (75.8 mg, 0.5 mmol), NH_4SCN (114 mg, 1.5 mmol), **[IrL2]Cl** (0.1 mol %), THF 5 mL, 24 h**.** White solid (75.3 mg, Isolated Yield: 72%). **^{1}H NMR (300 MHz, $CDCl_3$, 25 °C):** δ (s, 1H), 7.78 (d, *J* = 2.0 Hz, 1H), 7.57 (d, *J* = 2.9 Hz, 1H), 7.37 (d, *J* = 8.7 Hz, 1H), 7.29 (d, *J* = 2.0 Hz, 1H) ppm.**MS EI(+) (CH_2Cl_2)**: m/z = 207.8 (208.0 calcd. for $[C_9H_5ClN_2S]^+$).

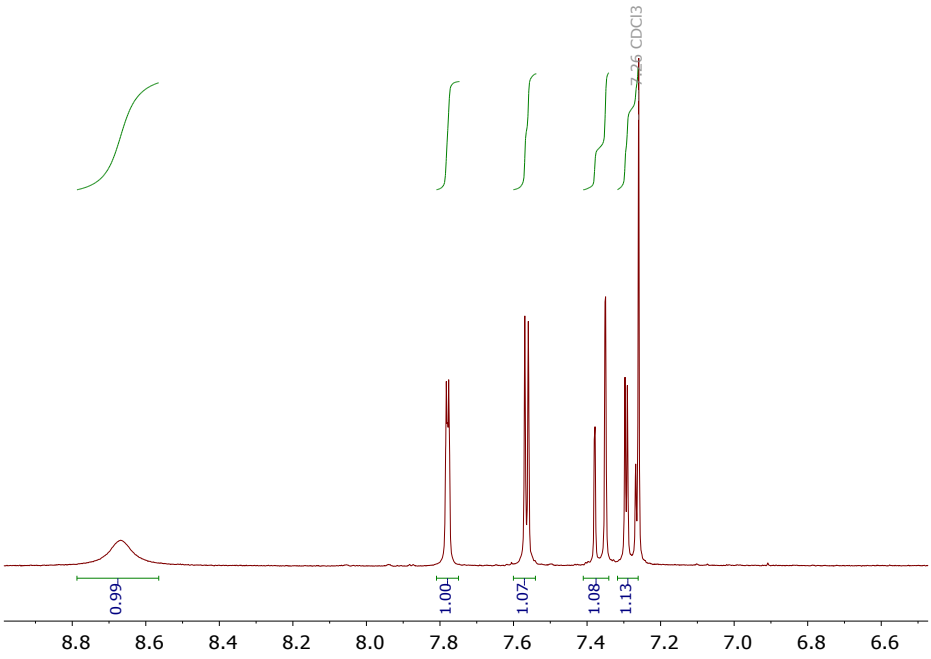

Figure S19. Aromatic area of the ^{1}H NMR (300 MHz, $CDCl_3$, 25 °C) spectrum of isolated **3c**.

5-bromo-3-thiocyanato-1H-indole (3d):

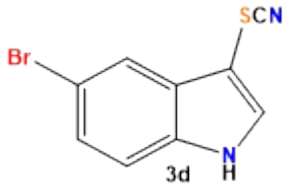

Reaction: 5-Bromo-1*H*-indole **2d** (98 mg, 0.5 mmol), NH_4SCN (114 mg, 1.5 mmol), **[IrL2]Cl** (0.1 mol %), THF 5 mL, 24 h. White solid (79.8 mg, Isolated Yield: 62%). **^{1}H NMR (300 MHz, $CDCl_3$, 25 °C):** δ 8.71 (s, 1H), 7.94 (d, *J* = 1.8 Hz, 1H), 7.55 (d, *J* = 2.9 Hz, 1H), 7.41 (dd, *J* = 8.7, 1.9 Hz, 1H), 7.32 (d, *J* = 8.7 Hz, 1H), 2.18 (s, 1H).**MS EI(+) (CH_2Cl_2)**: m/z = 251.8 (251.9 calcd. for $[C_9H_5BrN_2S]^+$) Da.

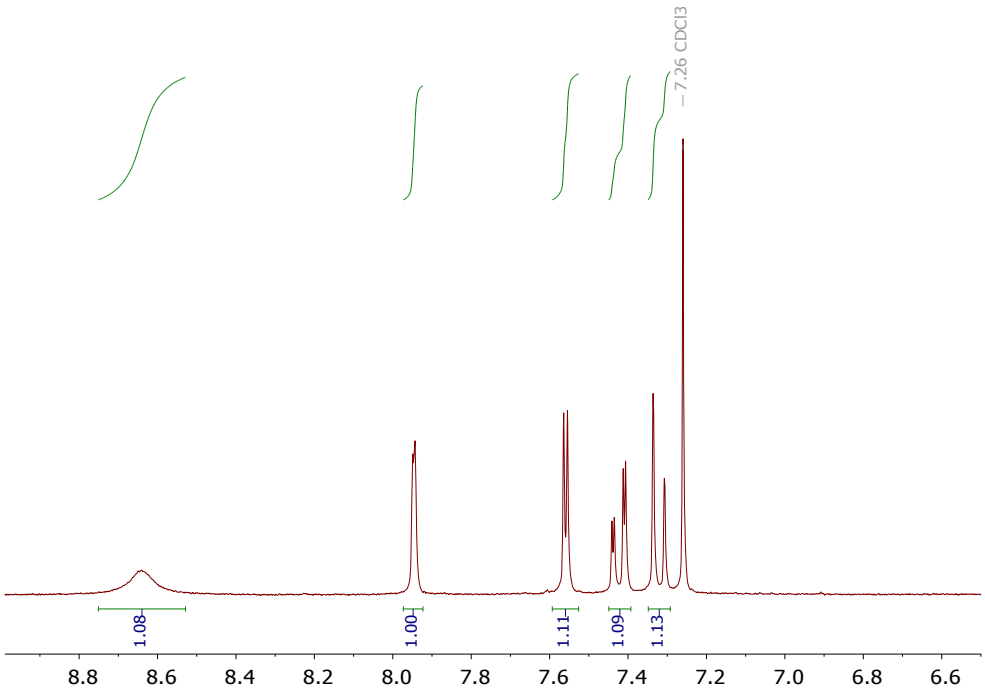

Figure S20. Aromatic area of the ^{1}HNMR (300 MHz, $CDCl_3$, 25 °C) spectrum of isolated **3d**.

6-chloro-3-thiocyanato-1H-indole (3e):

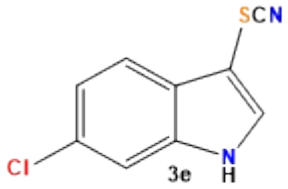

Reaction: 6-Choloro-1*H*-indole **2e** (75.8 mg, 0.5 mmol), NH_4SCN (114 mg, 1.5 mmol), **[IrL2]Cl** (0.1 mol %), THF 5 mL, 24 h**.** White solid (81,4 mg, Isolated Yield 78%). **^{1}H NMR (300 MHz, $CDCl_3$, 25 °C):** δ 8.60 (s, 1H), 7.72 (dt, *J* = 8.5, 0.7 Hz, 1H), 7.56 (d, *J* = 2.8 Hz, 1H), 7.46 (dd, *J* = 1.8, 0.6 Hz, 1H), 7.30 (dd, *J* = 8.5, 1.8 Hz, 1H).

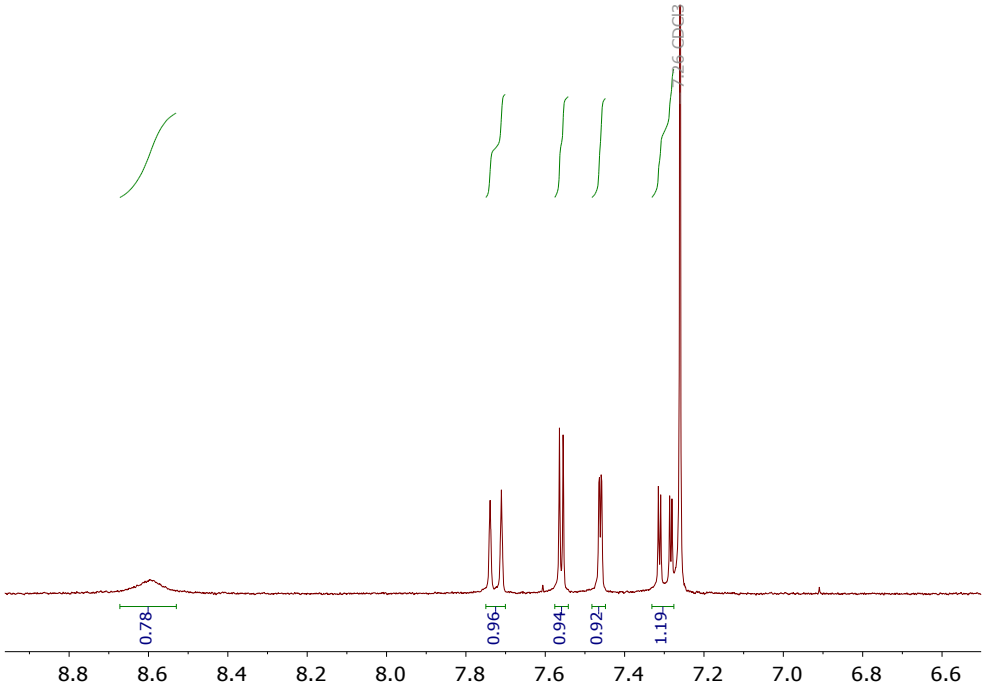

Figure S21. Aromatic area of the ^{1}H NMR (300 MHz, $CDCl_3$, 25 °C) spectrum of isolated **3e**.

5-methoxy-3-thiocyanato-1H-indole (3f):

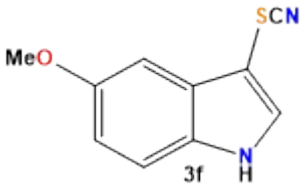

Reaction: 5-Methoxy-1*H*-indole **2f** (73.5 mg, 0.5 mmol), NH_4SCN (114 mg, 1.5 mmol), **[IrL2]Cl** (0.1 mol %), THF 5 mL, 24 h. White solid (100.1 mg, Isolated Yield 98%). **^{1}H NMR (300 MHz, $CDCl_3$, 25 °C):** δ 8.50 (s, 1H), 7.51 (d, *J* = 2.9 Hz, 1H), 7.33 (dd, *J* = 8.9, 0.6 Hz, 1H), 7.19 (d, *J* = 2.4 Hz, 1H), 6.97 (dd, *J* = 8.9, 2.4 Hz, 1H), 3.92 (s, 3H) ppm. **MS EI(+) (CH_2Cl_2)**: m/z = 203.8 (204.0 calcd. for $[C_{10}H_8N_2OS]^+$) Da.

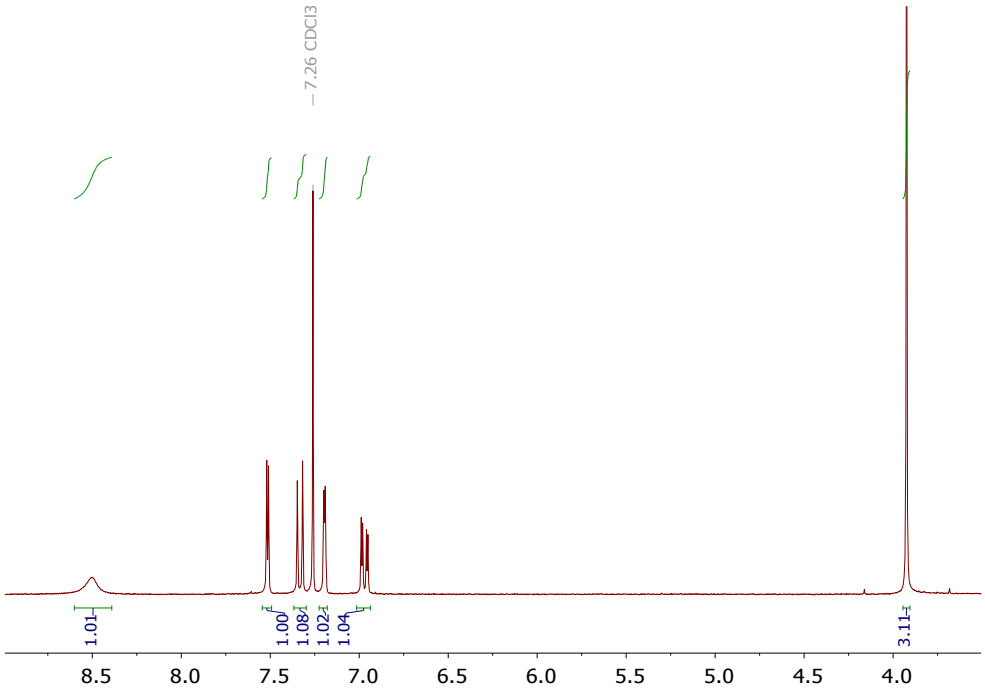

Figure S22. Aromatic area of the ^{1}H NMR (300 MHz, $CDCl_3$, 25 °C) spectrum of isolated **3f**.

N-methyl-3-thiocyanato-1H-indole (3g):

Reaction: 1-Methyl-indole **3g** (65.6 mg, 0.5 mmol), NH_4SCN (114 mg, 1.5 mmol), **[IrL2]Cl** (0.1 mol %), THF 5 mL, 24 h. Pale yellow solid (92.2 mg, Isolated Yield 97%). **^{1}H NMR (300 MHz,** $CDCl_3$**, 25 °C):** δ 7.84 – 7.76 (m, 1H), 7.44 – 7.29 (m, 4H), 3.84 (s, 3H) ppm. **MS EI(+) (CH_2Cl_2)**: m/z = 188.1 (188.0 calcd. for $[C_{10}H_8N_2S]^+$).

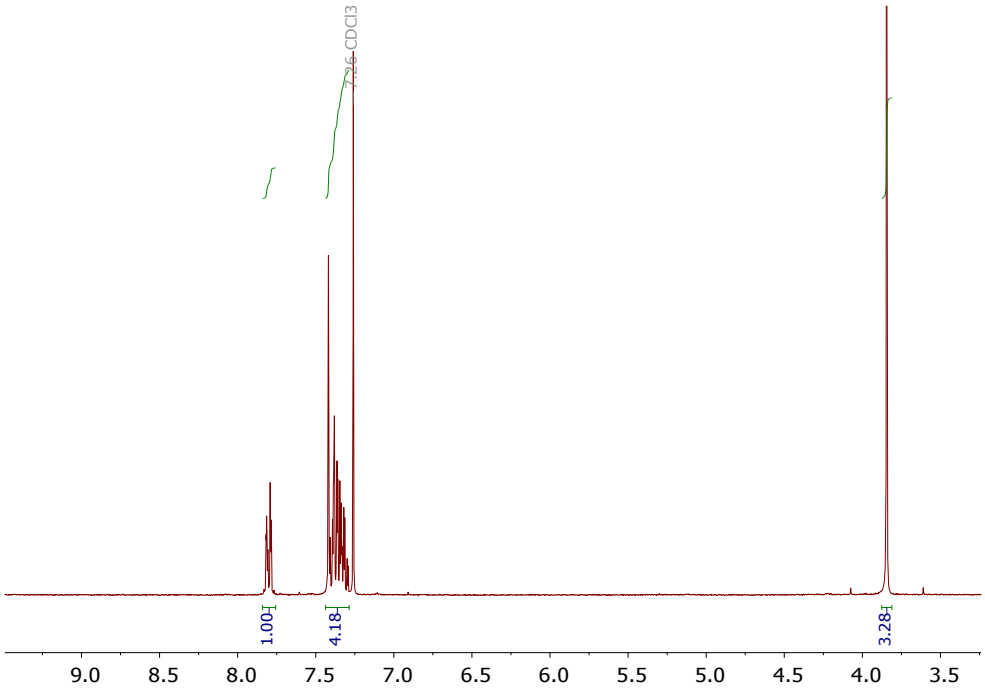

Figure S23. ^{1}H NMR (300 MHz, $CDCl_3$, 25 °C) spectrum of isolated **3g**.

2-methyl-3-thiocyanato-1H-indole (3h):

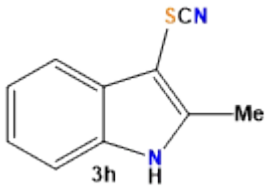

Reaction: 2-Methyl-1*H*-indole **2h** (65.6 mg, 0.5 mmol), NH_4SCN (114 mg, 1.5 mmol), **[IrL2]Cl** (0.1 mol %), THF 5 mL, 24 h. White solid (77.2 mg, **Isolated** Yield: 82%). **^{1}H NMR (300 MHz**, $CDCl_3$, **25 °C):** δ 8.39 (s, 1H), 7.75 – 7.66 (m, 1H), 7.38 – 7.30 (m, 1H), 7.30 – 7.22 (m, 2H), 2.61 (s, 3H). **MS EI(+) (CH_2Cl_2)**: m/z = 187.8 (188.0 calcd. for $[C_{10}H_8N_2S]^+$) Da.

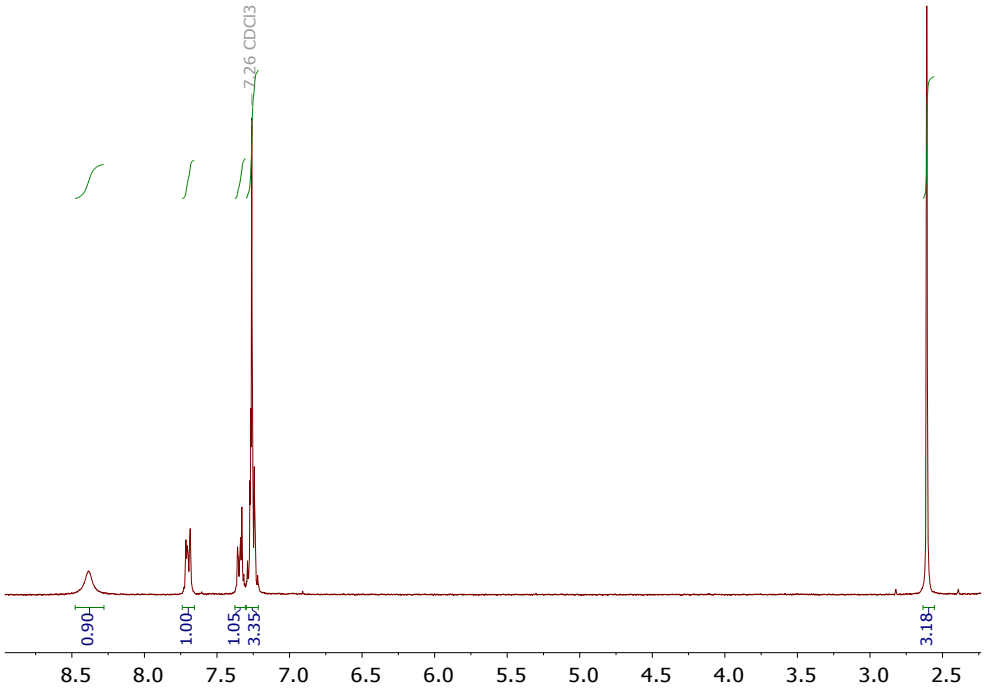

Figure S24. Aromatic area of the ^{1}H NMR (300 MHz, $CDCl_3$, 25 °C) spectrum of isolated **3h**.

9.- Photocatalytic Oxidative dehydrogenation experiments and ^{1}H NMR spectra of the crudes

Photo-Oxidative dehydrogenation from 1a to 2a

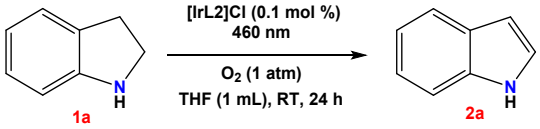

Reaction: 1*H*-Indoline **1a** (59.6 mg, 0.5 mmol), **[IrL2]Cl** (0.1 mol %), THF 5 mL**,** 24 h. **^{1}H NMR (300 MHz, $CDCl_3$, 25 °C):** δ 8.27 (bs, 1H), 7.66 (d, *J* = 8.2 Hz, 1H), 7.41 (dd, *J* = 8.0, 1.0 Hz, 1H), 7.24 – 7.19 (m, 2H), 7.16 – 7.09 (m,1H), 6.57 (m, 1H).

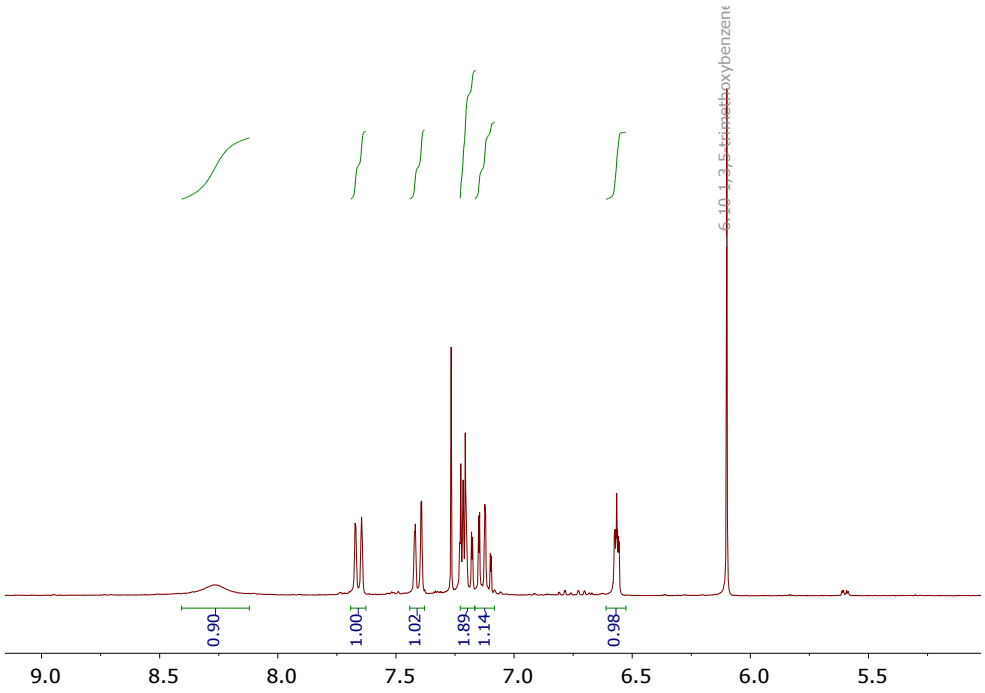

Figure S25. ^{1}H NMR (300 MHz, $CDCl_3$, 25 °C) spectrum for the crude of the oxidative dehydrogenation experiment from **1a** to **2a**.

Photo-oxidative dehydrogenation from 1b to 2b

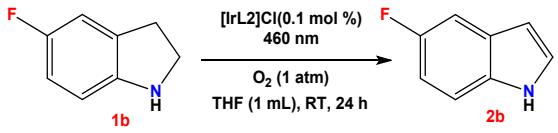

Reaction: 5-Fluoro-1*H*-indoline **1b** (68.6 mg, 0.5 mmol), **[IrL2]Cl** (0.1 mol %), THF 5 mL, 24 h**. ^{1}H NMR (300 MHz, $CDCl_3$, 25 °C)** δ 8.24 (bs, 1H), 7.37 – 7.22 (m, 3H), 6.95 (td, *J* = 9.1, 2.6 Hz, 1H), 6.53 (m, 1H).

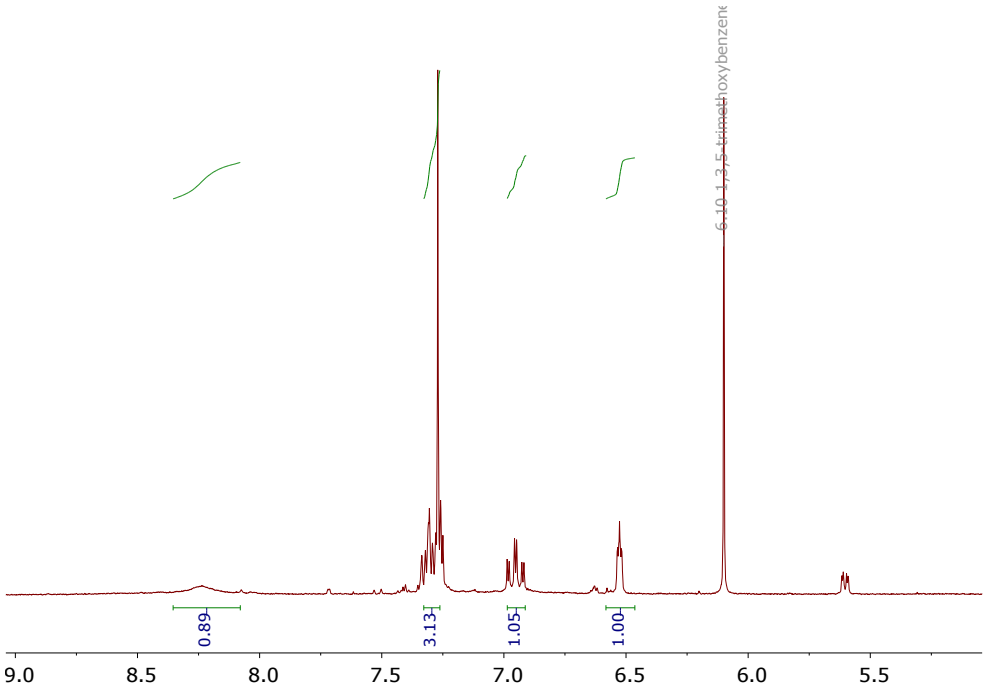

Figure S26. ^{1}H NMR (300 MHz, $CDCl_3$, 25 °C) spectrum for the crude of the oxidative dehydrogenation experiment from **1b** to **2b**.

Photo-Oxidative dehydrogenation from 1d to 2d

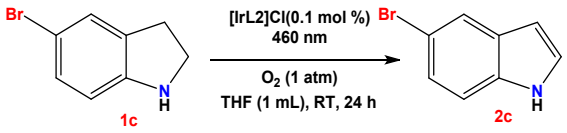

Reaction: 5-Bromo-1*H*-indoline **1c** (99 mg, 0.05 mmol), **[IrL2]Cl** (0.1 mol %), THF 5 mL, 24 h. **^{1}H NMR (300 MHz, $CDCl_3$, 25 °C)** δ 8.38 (s, 1H), 7.78 (s, 1H), 7.29–7.26 (m, 2H), 7.24-7.21 (m, 1H), 6.50 (m, 1H).

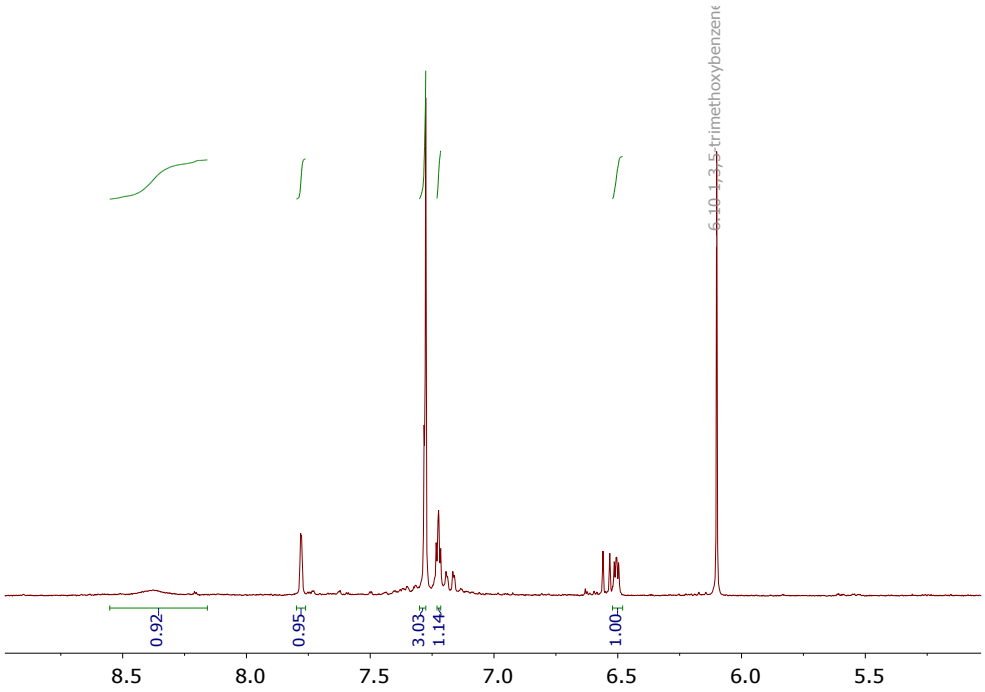

Figure S27. ^{1}H NMR (300 MHz, $CDCl_3$, 25 °C) spectrum for the crude of the oxidative dehydrogenation experiment from **1d** to **2d**.

Photo-Oxidative dehydrogenation from 1h to 2h

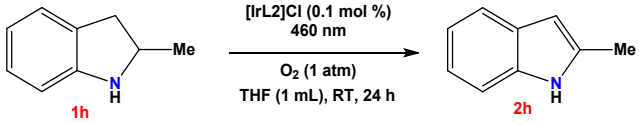

Reaction: 2-Methyl-1*H*-indoline **1h** (66.6 mg, 0.5 mmol), **[IrL2]Cl** (0.1 mol %), THF 5 mL, 24 h. **^{1}H NMR (300 MHz, $CDCl_3$, 25 °C)** δ 8.01 (bs, 1H), 7.51 (d, *J* = 7.1 Hz, 1H), 7.28 (d, *J* = 7.6 Hz, 1H), 7.20 – 7.02 (m, 2H), 6.22-6.21 (m, 1H), 2.45 (s, 3H, -Me).

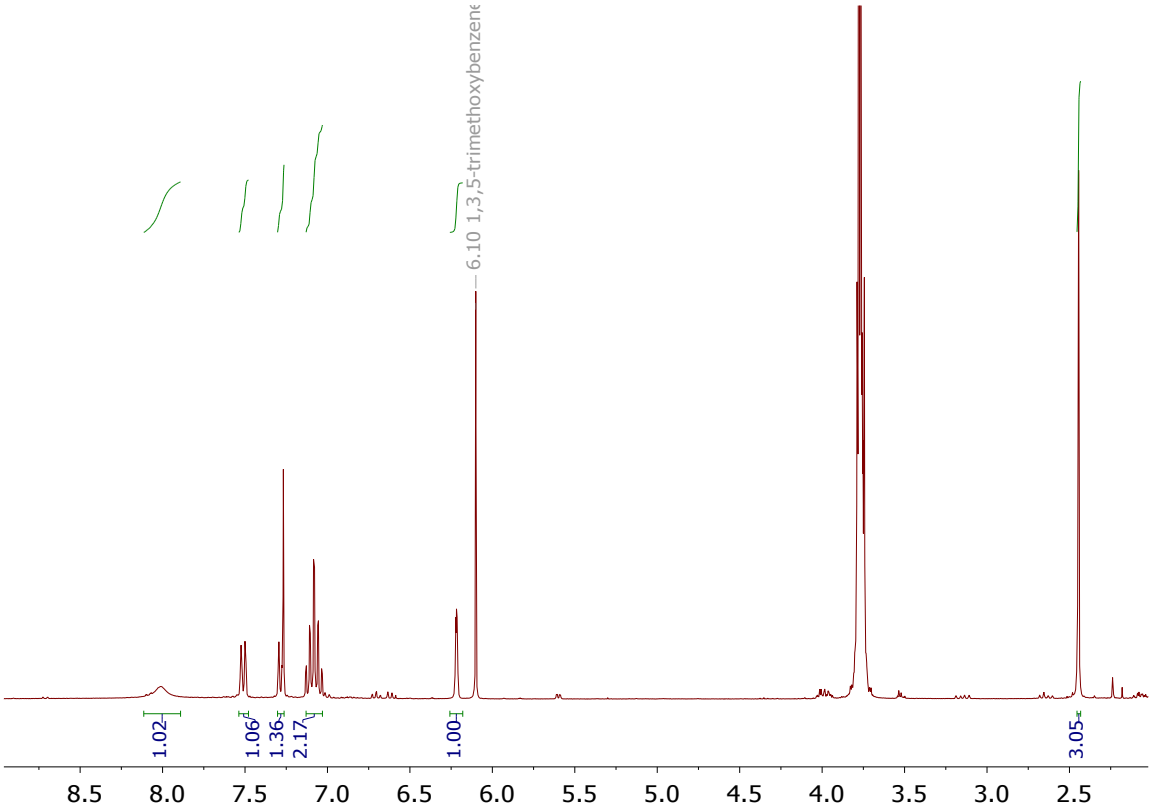

Figure S28. ^{1}H NMR (300 MHz, $CDCl_3$, 25 °C) spectrum for the crude of the oxidative dehydrogenation experiment from **1h** to **2h**.

10.- One-pot experiments and ^{1}H NMR spectra of the crudes

One-pot experiment from 1a to 3a

Reaction: 1*H*-Indoline **1a** (59.6 mg, 0.5 mmol), NH_4SCN (114 mg, 1.5 mmol), **[IrL2]Cl** (0.1 mol %), THF 5 mL, 48 h.

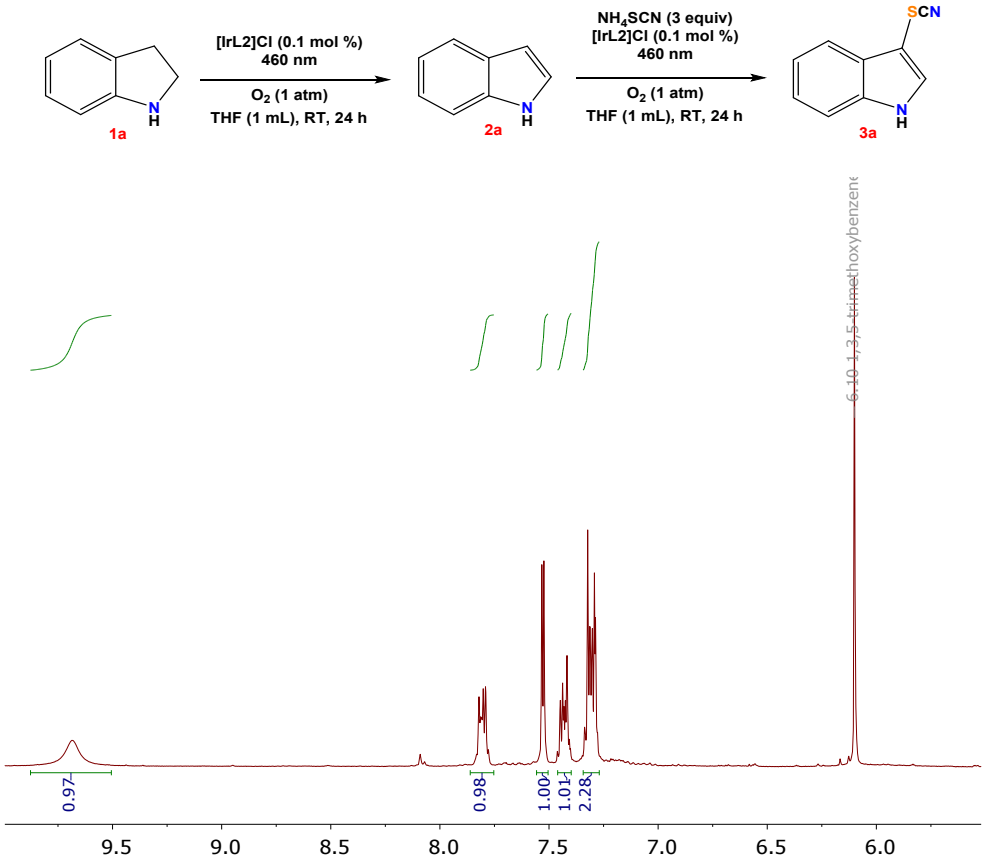

Figure S29. ^{1}H NMR (300 MHz, $CDCl_3$, 25 °C) spectrum for the crude of the one-pot experiment from **1a** to **3a**.

One-pot experiment for 1b to 3b

Reaction: 5-Fluoro-1*H*-indoline **1b** (68.6 mg, 0.5 mmol), NH_4SCN (114 mg, 1.5 mmol), **[IrL2]Cl** (0.1 mol %), THF 5 mL, 48 h.

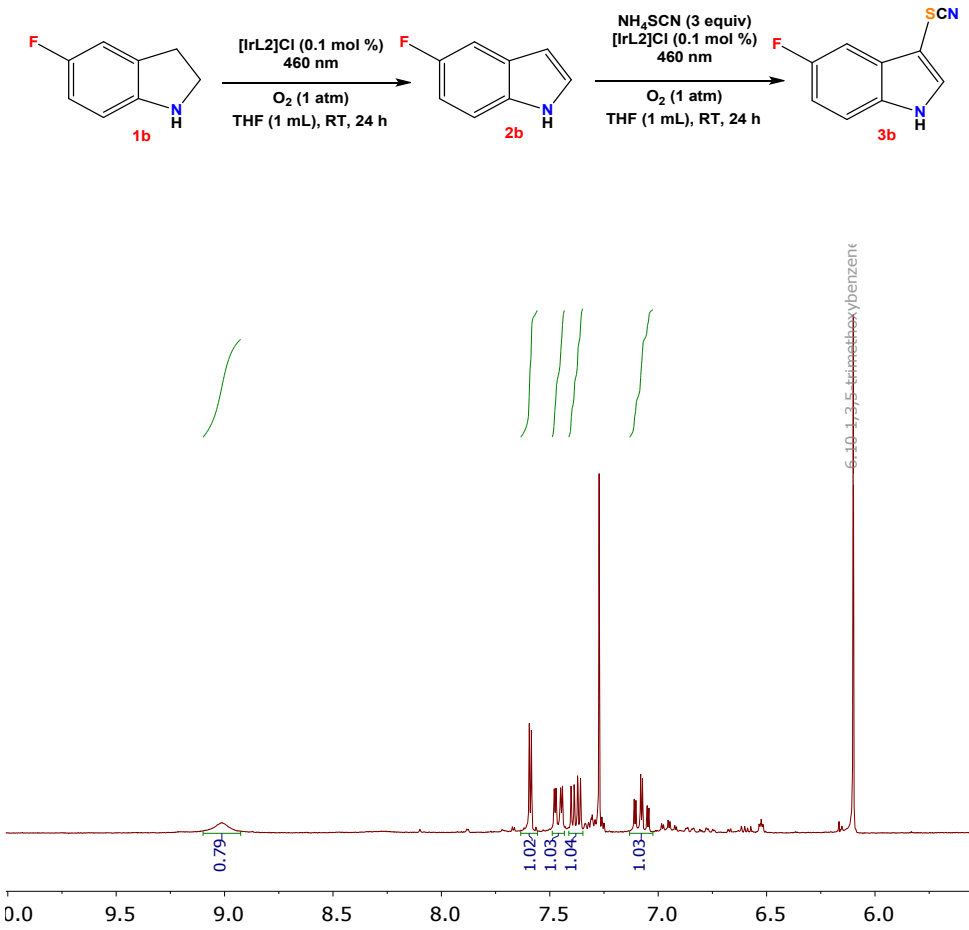

Figure S30. ^1H NMR (300 MHz, $CDCl_3$, 25 °C) spectrum for the crude of the one-pot experiment from **1b** to **3b**.

One-pot experiment for 1d to 3d

Reaction: 5-Bromo-1*H*-indoline **1d** (99 mg, 0.05 mmol), NH_4SCN (114 mg, 1.5 mmol), **[IrL2]Cl** (0.1 mol %), THF 5 mL, 24 h.

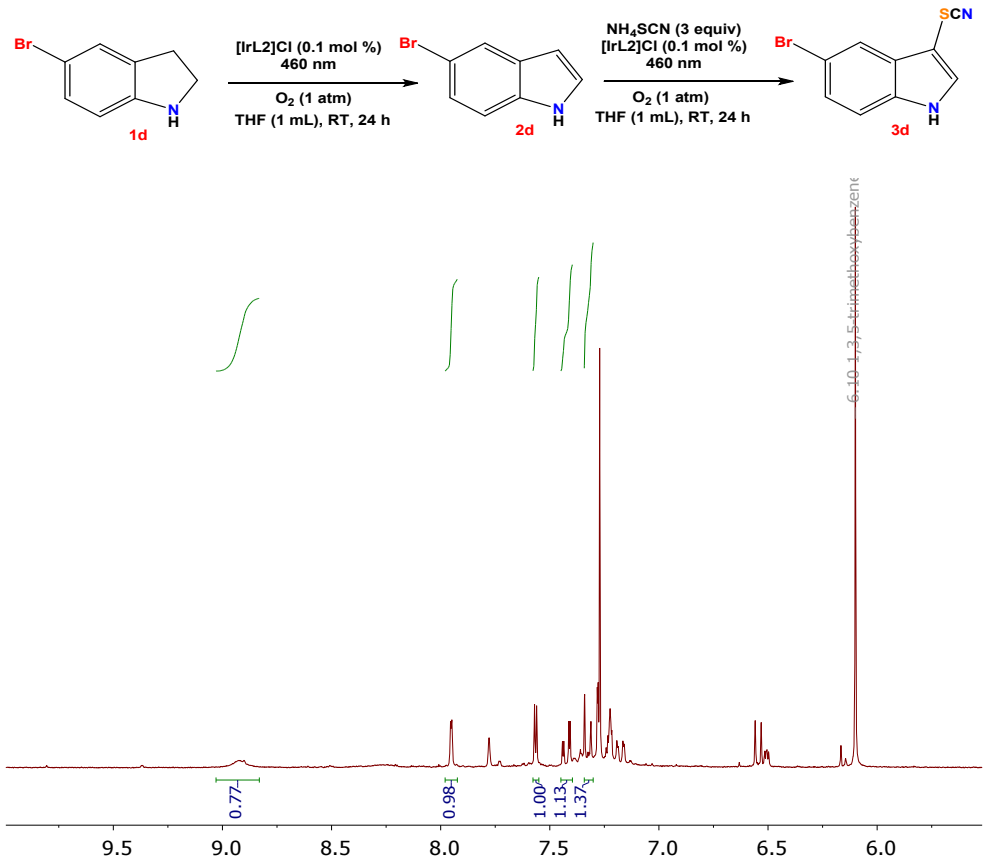

Figure S31. ^{1}H NMR (300 MHz, CDCl3, 25 °C) spectrum for the crude of the one-pot experiment from **1d** to **3d**.

One-pot experiment from 1h to 3h

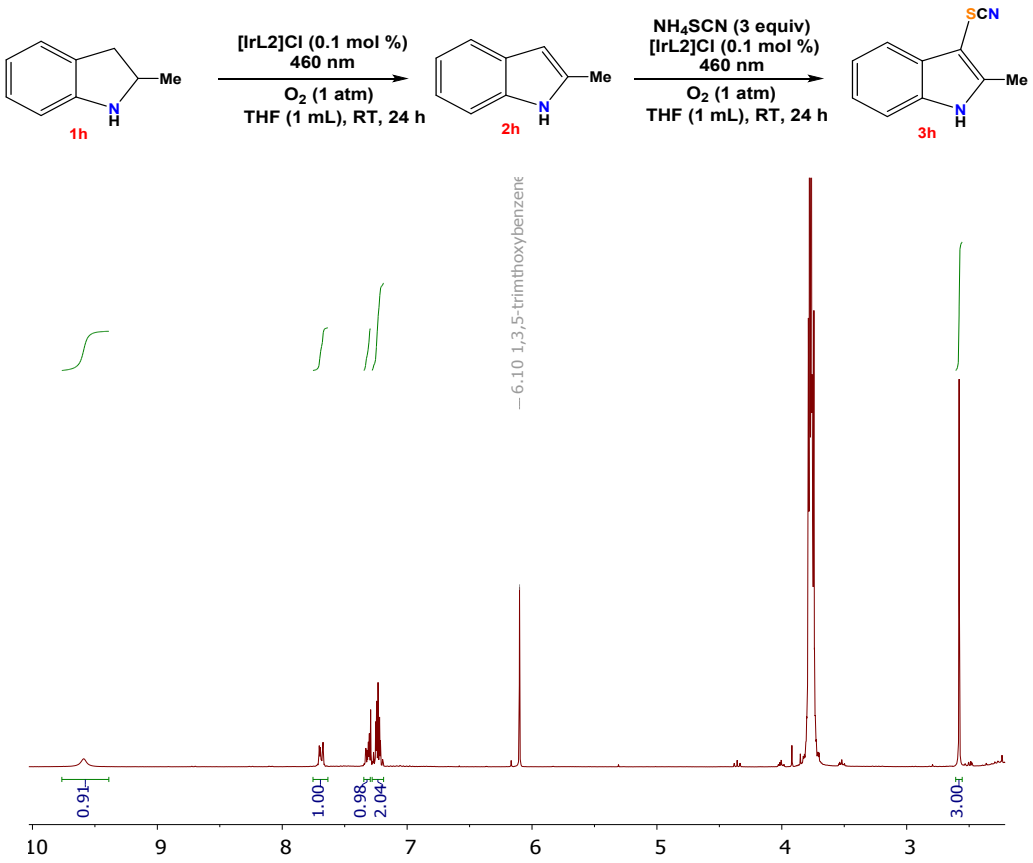

Figure S32. ^{1}H NMR (300 MHz, $CDCl_3$, 25 °C) spectrum for the crude of the one-pot experiment from **1h** to **3h**.

11.- Gram-scale in the one-pot process from 1a to 3a

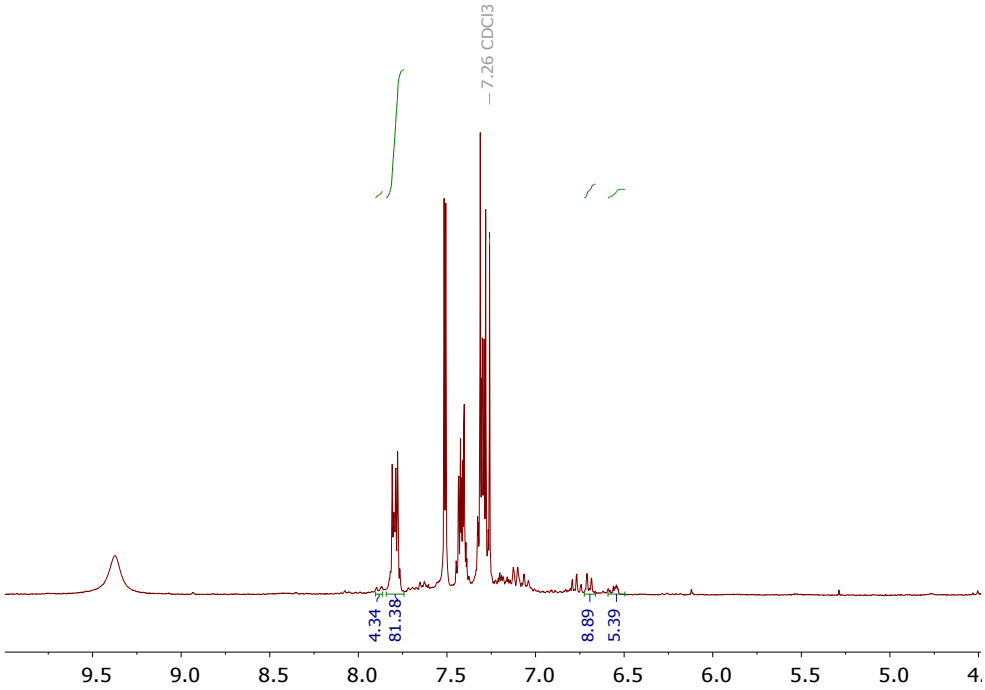

Figure S33. ^{1}H NMR (300 MHz, $CDCl_3$, 25 °C) spectrum for the crude of the gram scale in the one-pot experiment from **1a** to **3a**.

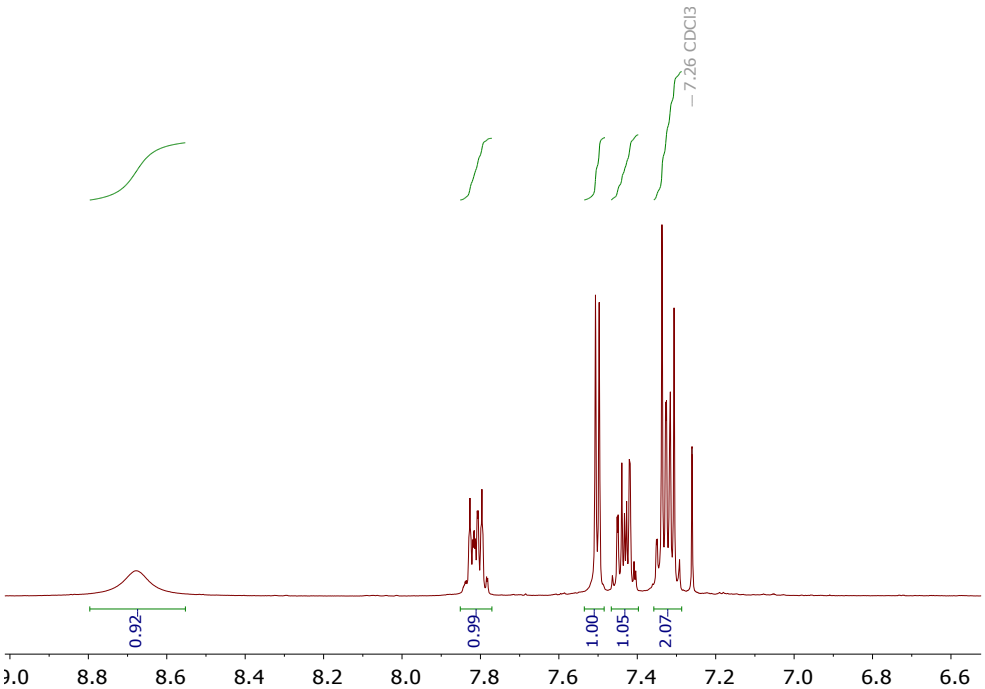

Figure S34. ^{1}H NMR (300 MHz, $CDCl_3$, 25 °C) spectrum for the product **3a** isolated in the gram-scale experiment from **1a**.

12.- Transient Absorption Spectroscopy Measurements

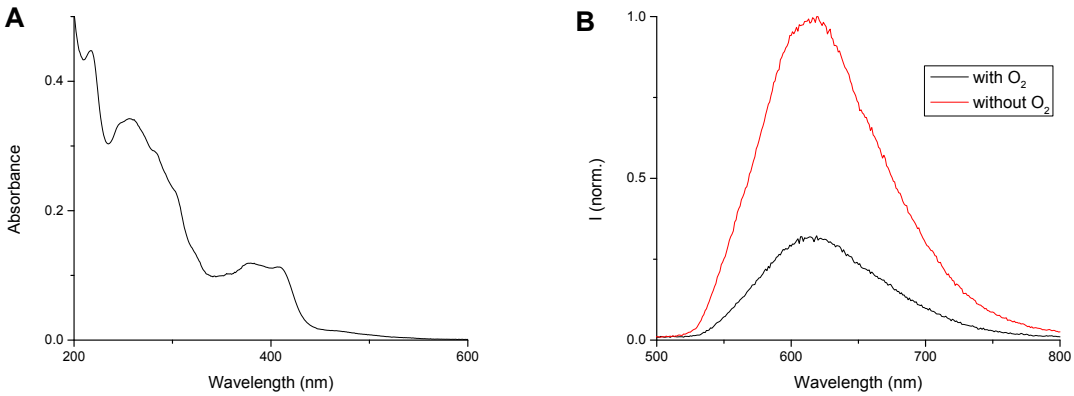

Figure S35. **(A)** Absorption and **(B)** Emission spectra (λ_{exc} = 355 nm) of Iridium complex **[IrL1]Cl** ($7.6x10^{-6}$ M) in acetonitrile at room temperature, aerated (black) and degassed (red) conditions.

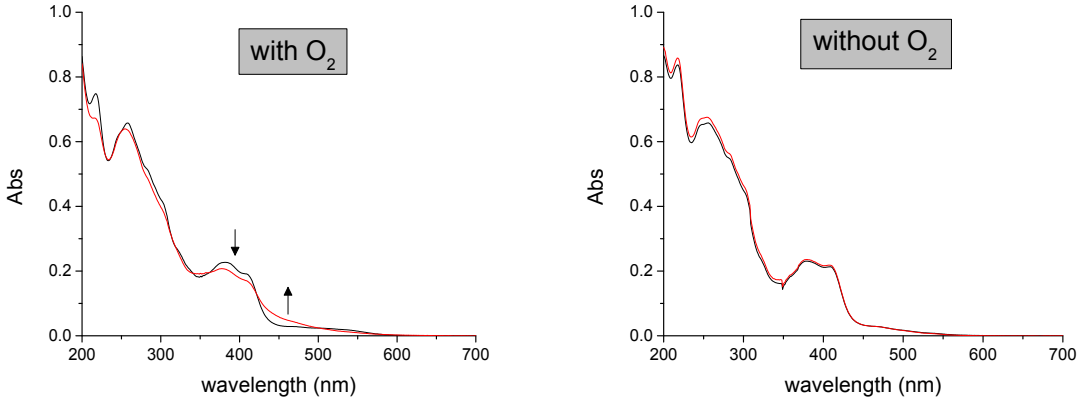

Figure S36. Absorption spectra of **[IrL1]Cl** in acetonitrile (1.41×10^{-5} M), in the presence (left) and absence (right) of oxygen, before (black) and after (red) laser flash-photolysis experiments.

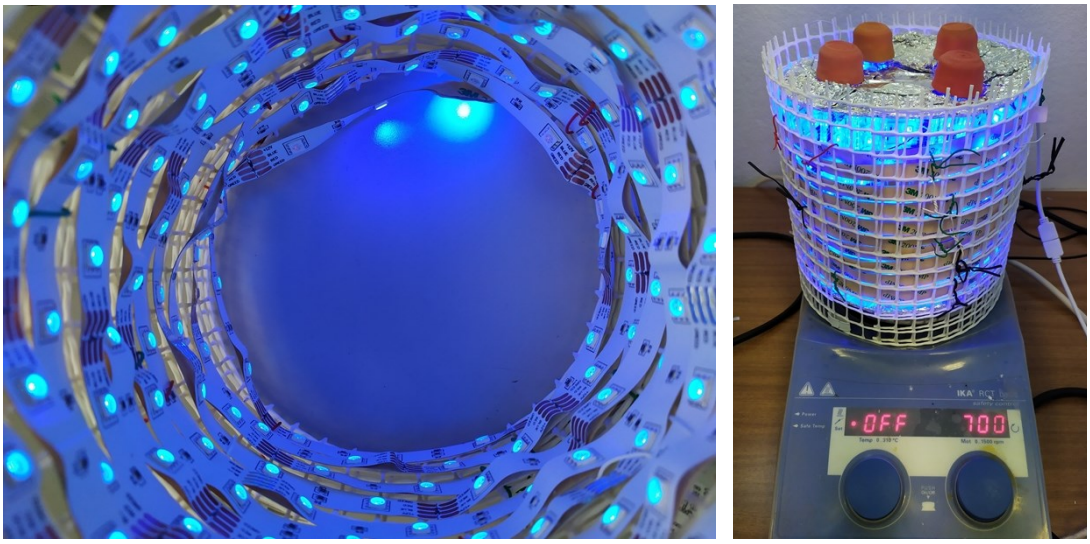

Figure S37. Experimental set-up for the standard photocatalytic experiments. 20 mL test tubes equipped with magnetic stirring and external blue light irradiation (LED strip, 5 m, λ_{ex} = 460 nm, 23 W) were used for these experiments. (A) Source irradiation source viewed from above. (B) Experimental set-up.

Figure S38. Experimental set-up for the gram-scale experiment corresponding to the one-pot photocatalytic conversion of **1a** into **3a**. A 250 mL three-neck round-bottom flask equipped with magnetic stirring and with external blue light irradiation (LED strip, 5 m, λ_{ex} = 460 nm, 23 W) was used for this experiment.

13.- REFERENCES

(1) Sprouse, S.; King, K. A.; Spellane, P. J.; Watts, R. J. Photophysical Effects of Metal-Carbon .Sigma. Bonds in Ortho-Metalated Complexes of Iridium(III) and Rhodium(III). *J. Am. Chem. Soc.* **1984**, *106* (22), 6647–6653.

(2) Fulmer, G. R.; Miller, A. J. M.; Sherden, N. H.; Gottlieb, H. E.; Nudelman, A.; Stoltz, B. M.; Bercaw, J. E.; Goldberg, K. I. NMR Chemical Shifts of Trace Impurities: Common Laboratory Solvents, Organics, and Gases in Deuterated Solvents Relevant to the Organometallic Chemist. *Organometallics* **2010**, *29* (9), 2176–2179.

(3) SAINT v8.37. Bruker-AXS (2016), APEX3 v2016.1.0.: Madison, Wisconsin, USA.

(4) Krause, L.; Herbst-Irmer, R.; Sheldrick, G. M.; Stalke, D. Comparison of Silver and Molybdenum Microfocus X-Ray Sources for Single-Crystal Structure Determination. *J. Appl. Crystallogr.* **2015**, *48* (1), 3–10.

(5) Farrugia, L. J. WinGX and ORTEP for Windows : An Update. *J. Appl. Crystallogr.* **2012**, *45* (4), 849–854.

(6) Sheldrick, G. M. SHELX-2014, Program for Crystal Structure Refinement. University of Göttingen: Göttingen, Germany 2014.

(7) Yang, R.; Yue, S.; Tan, W.; Xie, Y.; Cai, H. DMSO/t-BuONa/O2 -Mediated Aerobic Dehydrogenation of Saturated N -Heterocycles. *J. Org. Chem.* **2020**, *85* (11), 7501–7509.

(8) Becke, A. D. DENSITY-FUNCTIONAL THERMOCHEMISTRY .3. THE ROLE OF EXACT EXCHANGE. *J.*

Chem. Phys. **1993**, *98* (7), 5648–5652.

(9) Lee, C. T.; Yang, W. T.; Parr, R. G. DEVELOPMENT OF THE COLLE-SALVETTI CORRELATION-ENERGY FORMULA INTO A FUNCTIONAL OF THE ELECTRON-DENSITY. *Phys. Rev. B* **1988**, *37* (2), 785–789.

(10) Grimme, S.; Antony, J.; Ehrlich, S.; Krieg, H. A Consistent and Accurate Ab Initio Parametrization of Density Functional Dispersion Correction (DFT-D) for the 94 Elements H-Pu. *J. Chem. Phys.* **2010**, *132* (15), 154104.

(11) Grimme, S.; Ehrlich, S.; Goerigk, L. Effect of the Damping Function in Dispersion Corrected Density Functional Theory. *J. Comput. Chem.* **2011**, *32* (7), 1456–1465.

(12) Francl, M. M.; Pietro, W. J.; Hehre, W. J.; Binkley, J. S.; Gordon, M. S.; DeFrees, D. J.; Pople, J. A. Self-Consistent Molecular Orbital Methods. XXIII. A Polarization-Type Basis Set for Second-Row Elements. *J. Chem. Phys.* **1982**, *77* (7), 3654–3665.

(13) Hay, P. J.; Wadt, W. R. Ab Initio Effective Core Potentials for Molecular Calculations. Potentials for K to Au Including the Outermost Core Orbitals. *J. Chem. Phys.* **1985**, *82* (1), 299–310.

(14) Marenich, A. V; Cramer, C. J.; Truhlar, D. G. Universal Solvation Model Based on Solute Electron Density and on a Continuum Model of the Solvent Defined by the Bulk Dielectric Constant and Atomic Surface Tensions. *J. Phys. Chem. B* **2009**, *113* (18), 6378–6396.

(15) Neese, F. The ORCA Program System. *WIREs Comput. Mol. Sci.* **2012**, *2* (1), 73–78.

(16) Neese, F. Software Update: The ORCA Program System, Version 4.0. *WIREs Comput. Mol. Sci.* **2018**, *8* (1).

(17) Fan, W.; Yang, Q.; Xu, F.; Li, P. A Visible-Light-Promoted Aerobic Metal-Free C-3 Thiocyanation of Indoles. *J. Org. Chem.* **2014**, *79* (21), 10588–10592.